

## Full length article

## The Egyptian geomagnetic reference field to the Epoch, 2010.0



H.A. Deebes, E.M. Abd Elaal\*, T. Arafa, A. Lethy, A. El Emam, E. Ghamry, H. Odah

Geomagnetic and Electric Department, National Research Institute of Astronomy and Geophysics., Egypt

## ARTICLE INFO

## Article history:

Received 8 November 2016

Revised 15 March 2017

Accepted 17 March 2017

Available online 3 May 2017

## ABSTRACT

The present work is a compilation of two tasks within the frame of the project “Geomagnetic Survey & Detailed Geomagnetic Measurements within the Egyptian Territory” funded by the “Science and Technology Development Fund agency (STDF)”. The National Research Institute of Astronomy and Geophysics (NRIAG), has conducted a new extensive land geomagnetic survey that covers the whole Egyptian territory. The field measurements have been done at 3212 points along all the asphalted roads, defined tracks, and ill-defined tracks in Egypt; with total length of 11,586 km. In the present work, the measurements cover for the first time new areas as: the southern eastern borders of Egypt including Halayeb and Shlatin, the Quattara depression in the western desert, and the new roads between Farafra and Baharia oasis. Also marine geomagnetic survey have been applied for the first time in Naser lake.

Misallat and Abu-Simble geomagnetic observatories have been used to reduce the field data to the Epoch 2010. During the field measurements, whenever possible, the old stations occupied by the previous observers have been re-occupied to determine the secular variations at these points.

The geomagnetic anomaly maps, the normal geomagnetic field maps with their corresponding secular variation maps, the normal geomagnetic field equations of the geomagnetic elements (EGRF) and their corresponding secular variations equations, are outlined. The anomalous sites, as discovered from the anomaly maps are, only, mentioned. In addition, a correlation between the International Geomagnetic Reference Field (IGRF) 2010.0 and the Egyptian Geomagnetic Reference Field (EGRF) 2010 is indicated.

© 2017 Production and hosting by Elsevier B.V. on behalf of National Research Institute of Astronomy and Geophysics. This is an open access article under the CC BY-NC-ND license (<http://creativecommons.org/licenses/by-nc-nd/4.0/>).

## 1. Introduction

The geomagnetic field is the sum of magnetic fields from several sources: the main field created by electric currents flowing in the Earth's core and is subjected to secular variation, the crustal field due to magnetization of rocks, external fields caused by electric currents flowing in the ionosphere and the magnetosphere, and induction fields due to electric currents induced in the Earth's crust and mantle by the time variations of the external fields. The geomagnetic field is usually presented (Chapman and Bartels, 1940; Parkinson, 1983; Campbell, 1997) by a potential equation:

$$V(r, \theta, \phi, t) = a \sum_{n=1}^N \left(\frac{a}{r}\right)^{n+1} \times \sum_{m=0}^n P_n^m(\theta) (g_n^m(t) \cos m\phi + h_n^m(t) \sin m\phi) \quad (1)$$

where  $(\theta)$  and  $(\phi)$  are geocentric colatitudes and longitudes,  $(r)$  is the radial coordinate,  $(a)$  is the spherical Earth's radius,  $P_n^m(\theta)$  is an associated Legendre polynomial with Schmidt's normalization, and the entire sum is called Spherical Harmonic Expansion (SHE),  $g_n^m$  and  $h_n^m$  are suitable coefficient, named Gauss elements of terrestrial magnetism, the two summation indices  $(n)$  and  $(m)$  are called degree and order respectively, and the maximum degree  $(N)$  being considered depends on the quality and amount of the observational database.

The geocentric components of the main geomagnetic field components are derived (Barraclough, 1987) by partial differentiation of Eq. (1)

$$X = \frac{1}{r} \frac{\partial V}{\partial \theta}, \quad Y = \frac{-1}{r \sin \theta} \frac{\partial V}{\partial \phi}, \quad Z = \frac{\partial V}{\partial r} \quad (2)$$

where  $(X, Y)$  and  $(Z)$  denote the northward, eastward and radially inward components respectively, of the field. In the case of the

\* Corresponding author.

E-mail address: [esmatabd@yahoo.com](mailto:esmatabd@yahoo.com) (E.M. Abd Elaal).

Peer review under responsibility of National Research Institute of Astronomy and Geophysics.



secular variation ( $X'$ ,  $Y'$  and  $Z'$ ) are to be regarded as representing the time rates of change of the quantities referred to above.

For some applications, the declination  $D$ , the inclination  $I$ , the horizontal intensity  $H$ , and the total intensity  $F$  are required. These components are calculated from  $X$ ,  $Y$ , and  $Z$  using the relations,

$$H = \sqrt{X^2 + Y^2}, \quad F = \sqrt{X^2 + Y^2 + Z^2}, \quad D = \arctan(Y/X), \\ I = \arctan(Z/H) \quad (3)$$

The accurate estimation of magnetic anomalies requires effective removal of the core and the external field components from the magnetic observations. Since continuous geomagnetic records in Egypt are sparse and not well-distributed, there is a clear need to improve the accuracy of the core field (Normal Field) and its secular variation. The geomorphologic conditions in Egypt limit the presence of man and the capability of installing, running, and preserving conventional geomagnetic observatories for continuous recording of the geomagnetic field. Now NRIAG have the new Abu-Simble observatory equipped by automatic instruments that are checked twice a year for maintenance. Its data is transferred to the head quarter at NRIAG by satellites.

In spite of the small number of the permanent stations (2 observatories) and their spatial distribution, and the field measurements that are limited mostly along the asphalted roads, defined tracks, and ill-defined tracks, yet the collected observations represent a precious ensemble that is important to monitoring the secular variation. In fact, the repeat stations are not many; however, in combination with other land surveys that reflect single occupations of sites, they can help to fill in some gaps both in sites and time for enhanced reconstruction of the secular variation.

In case of relatively small area, many authors (e.g. Bucha, 1957; Fahim, 1968) found that it is satisfactory to drive the core field (the normal field)  $T(x,y)$  and its secular variation by adopting one central point to which all the reductions can be done by applying Taylor's Expansion

$$T(x,y) = a_0 + b_1(x - x_0) + b_2(y - y_0) + c_1(x - x_0)^2 \\ + c_2(x - x_0)(y - y_0) + c_3(y - y_0)^2 \quad (4)$$

where ( $a_0$ ) represents the value of the element at the central point, ( $b_1$ ,  $b_2$ ,  $c_1$ ,  $c_2$ , and  $c_3$ ) are the coefficients of the expansion, and ( $x_0$ ,  $y_0$ ) represent the coordinates of the central point. In the present work, each value of geomagnetic element measured in the field is used in a quadratic function of Taylor's Expansion depending on the site's latitude and longitude, considering El-Minia (Latitude 28°06.3' N & Longitude 30°45.5' E) as a central point.

## 2. Geomorphology and geology of Egypt

Egypt occupies the north eastern corner of Africa, situated between latitudes 22° and 32° N and between longitudes 25° and 32° E, embraces a total area of almost one million km<sup>2</sup> (Fig. 1). The greatest part of Egypt consists of barren and desolate desert. The River Nile divides the country into two distinct morphological and geological regions: Western Desert & Eastern Desert. The Western Desert is essentially a plateau desert with vast expanses of rocky ground and numerous extensive and closed-in depressions. Its most important topographical features are Kharga, Farafra, Bahariya Oases, El-Gulf Elkabir plateau and the Arbaeen desert. The land to the east of the Nile forms one geomorphological region, it is divided into the Eastern Desert and Sinai Peninsula which separated from main land of Egypt by the Gulf of Suez and the Suez Canal. The Eastern Desert consists essentially of a backbone of high rugged mountains running parallel to and at a relatively short distance from the coast. Sinai Peninsula continuous with the Asiatic

continent. Its core consists of an intricate complex of high and very rugged igneous and metamorphic mountains.

The geology of Egypt includes rocks from the Archaean early Proterozoic times and on ward. These oldest rocks are found as inliers in Western Desert. In contrast, the rocks of the Eastern desert are largely late Proterozoic age. Through the country this older basements is overlain by Palaeozoic sedimentary rocks. Cretaceous rocks occur commonly whilst sediments indicative of repeated marine transgression and regression are characteristic of the Cenozoic (Said, 1990; Issawi et al., 1999).

In Sinai, the Paleozoic rocks were suggested for beds overlying the Precambrian basement in the southwestern Sinai. The Mesozoic strata crops out in northern Sinai where an almost complete sequence from Triassic to Cretaceous is known. The end of Oligocene witnessed the rifting movements that brought the gulf of Suez to its modern shape (Neev, 1975; Said, 1990; Abdelkhalek et al., 1993; Rabeh, 2003, and Deebes, 2012).

## 3. Historical review of the magnetic survey in Egypt

The first reliable magnetic survey in Egypt started by Captain Lyons (Lyons, 1910) between the years 1893 and 1901 at different places of the country. Also, the Pola Expedition headed by Rossler made other observations along the Red Sea Coast, during 1895–1898, on her way from the Mediterranean to the Indian Ocean. Results of these surveys were published by Keeling (1907). Later Hurst made a magnetic survey along the Nile Valley in Egypt and the Sudan in 80 points during 1908–1914. Using the results of the Pola Expedition together with his data, Hurst (1915) constructed magnetic maps showing the isogonic lines for Egypt and the Sudan to the Epoch 1910. During 1918, the Carnegie Institution of Washington during a world survey carried out some observations at some points in Egypt (Carnegie Institution, 1920). These results were used by Knox Shaw, together with the old data of 1910 to construct a Declination map to the Epoch 1920 then to the Epoch 1930 (Fig. 2). After that, Madwar made some repeat observations at the old Hurst stations along the Nile Valley and constructed a declination map to the Epoch 1940. He, also, made some field survey in the Sudan during 1952 (Madwar, 1954). During the period 1957–1966, and in view of the “World Magnetic Survey” plan sponsored by the I.A.G.A., Fahim performed absolute observations of the elements  $H$ ,  $Z$ ,  $D$  at 148 stations together with 861 points for the  $Z$  and  $H$  components distributed over the country (Fahim and Wienert, 1958). Fahim published the geomagnetic maps reduced to the Epoch 1965 (Fahim, 1968). Ibrahim (1971) used Fahim's data with the old observations and produced the normal geomagnetic field of U.A.R. for the Epoch 1965 and its secular variations. Then, since 1970 until now, the members of the geomagnetic department in NRIAG have performed detailed surveys at separated parts of Egypt e.g. (Deebes et al., 1978; Deebes and Ahmed, 1979, and Deebes et al., 1980).

## 4. The present magnetic survey to Epoch 2010.0

During the period 2010–2011, the land Geomagnetic survey for the Whole Territory of Egypt is conducted by three missions conducted to measure the geomagnetic elements  $F$ ,  $I$ , and  $D$  in the Egyptian territory (Western Desert, Eastern Desert, Nile Valley, Sinai, and Naser lake). The following considerations are followed In each trip: (a) Misallat geomagnetic observatory (29.51444°N, 30.889525°E) is considered as a tying point for the field measurements at the northern part of Egypt. (b) Abu-Simble geomagnetic observatory (22.489672°N, 31.544821°E) is considered as a tying point for the measurements at the southern part of Egypt. (c) Five subsequent measurements are done at each point of observation to



**Fig. 1.** Geographical map of Egypt.



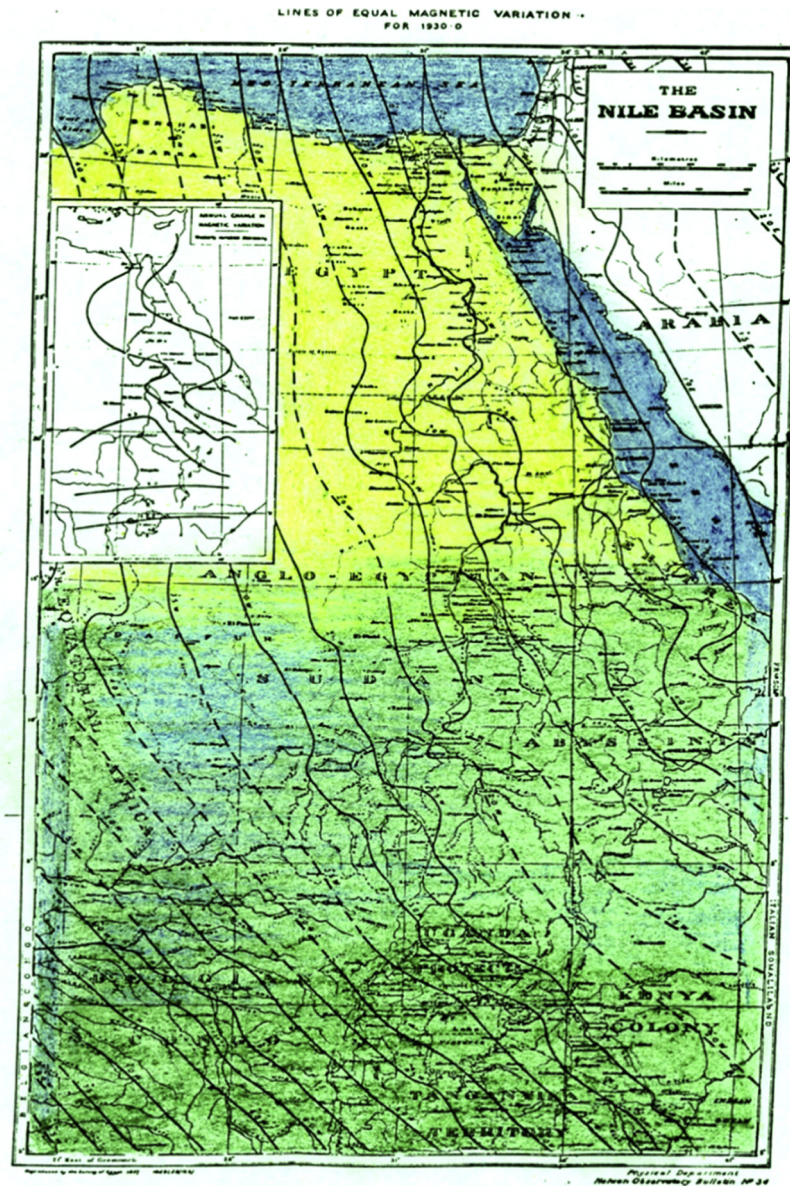


Fig. 2. Lines of equal magnetic variation for 1930.

assure the homogeneity of the place and the accuracy of the obtained geomagnetic values. If the readings of the magnetometers are not fitting together, the observer moves about 100 meter apart and repeats the measurements till he obtains consistent readings, (d) the observer always avoids measurements near any source of artificial disturbances by at least  $\frac{1}{2}$  km. These sources may be the canals as the Nile silt cause disturbance of about 30 nT, the rail way lines, the high tension electric lines, the existing pipe lines under the ground, the buried electric cables, and the high way roads, (e) the observer draws a sketch for the site to help in reoccupying the site in future, and (f) the observer puts a scientific notes for each point of observation concerning the geological nature and structure, and the volcanic and basaltic eruptions. These information help in the interpretation of the geomagnetic data.

The absolute measurements have been performed at what is called “Absolute Stations” each 20–15 km. apart (Fig. 3), along all the asphalted roads, defined tracks, and ill-defined tracks in the whole country, where the total field intensity (F), the Declination (D) and the Inclination (I) are measured. Traveling from one absolute station to the next one, (F) is measured each 2–5 km. apart according to the differences in the subsequent measurements.

The equipment used during the survey consist of: (a) two proton magnetometers to measure the total geomagnetic intensity, (b) one axis D/I fluxgate magnetometer to measure the absolute declination and inclination of the geomagnetic field, (c) GPS to determine the geographical coordinates of the observed points, (d) G-882 Marine Magnetometer (Fig. 4), (e) non-magnetic tent/umbrella to protect the equipment from sun shining or rain during the measurements, and (g) Geological maps (scale 1:10,000) of Egypt showing also the asphalted roads, the defined, and the ill-defined tracks.

## 5. The measurements and computation of the magnetic elements

At the absolute stations, the proton magnetometer is used to measure the total magnetic intensity, while D/I magnetometer is used to determine the magnetic inclination, the geomagnetic meridian, and the geographical meridian.

To determine the angle of Declination, Sun azimuth and declination, (Fig. 5), measurements are applied to specify the geo-



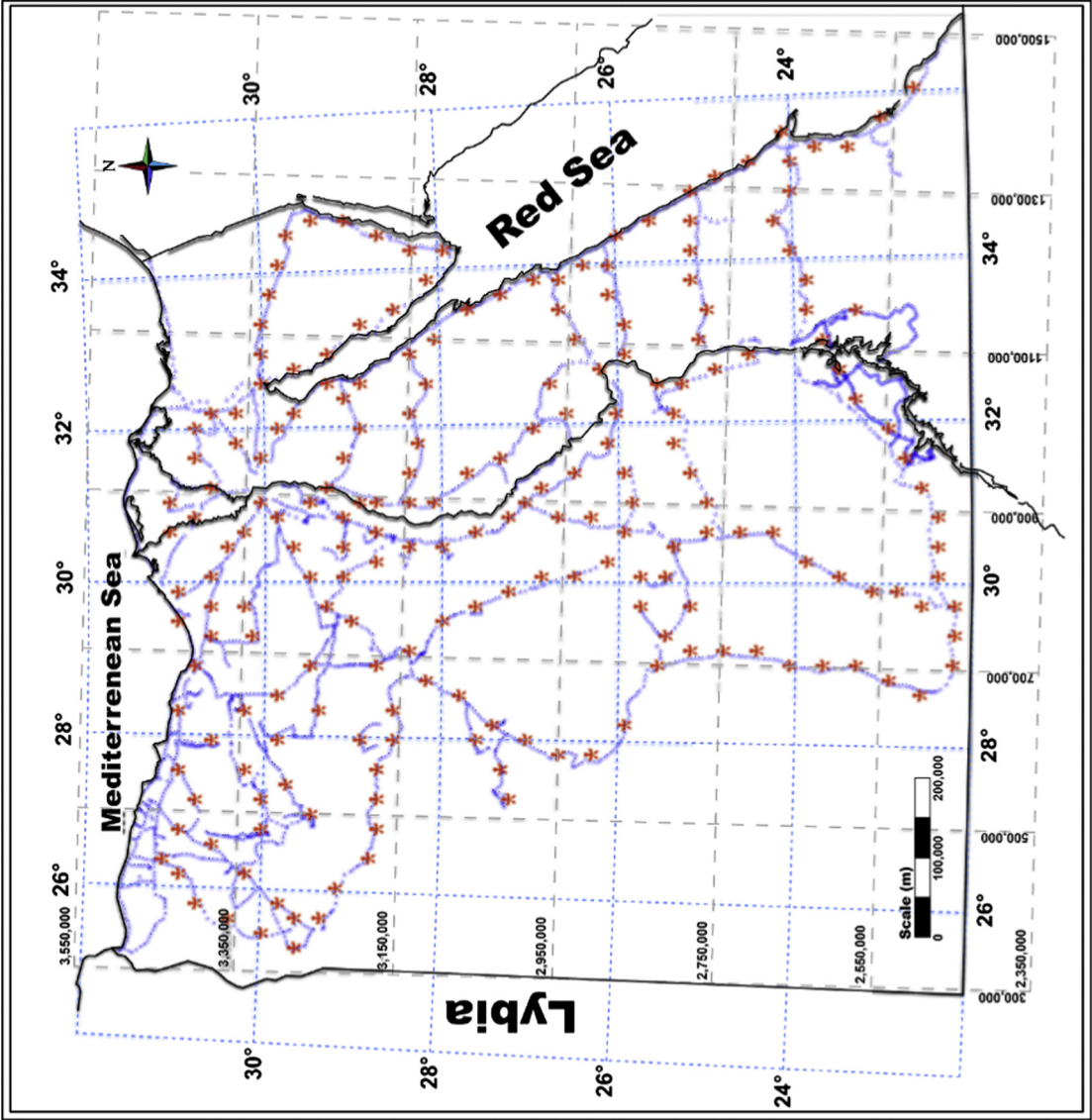


Fig. 3. The location of the absolute geomagnetic measurements.



Fig. 4. Marine survey using G-882 Marine.

graphic and the magnetic meridians. The azimuth of a chosen reference mark within the area of the observation is calculated before and after 8 successive solar observations on the solar limb (Wienert, 1970). The equation for the determination of the Sun's azimuth is:

$$\cot(A) = [\cos(H) \sin(\phi) - \cos(\phi) \tan(\delta)] / \sin(H) \quad (5)$$

where ( $A$ ) is Sun azimuth, ( $H$ ) is solar hour angle, ( $\delta$ ) is solar declination and ( $\phi$ ) is the latitude of the place. Both Sun azimuth and declination observations have been referred to the index mark to determine the geomagnetic Declination.

The magnetic recordings of Misallat and Abu-Simble observatories, or the field base stations, have been used to reduce the field data for the daily variation by subtracting the corresponding element value at the observatory from that measured in the field at the same time. The two observatories have been, also, used to reduce the data to the Epoch 2010.0. The absolute values of Misallat and Abu-Simble for the Epoch 2010 are taken as the mean values of the monthly means of the months from July 2009 to June 2010 for  $F$ ,  $D$ , and  $I$  elements. Then, for each element, the difference (station's value after reduction of the daily variations – observatory's value to the Epoch 2010.0) have been computed for all the field measured points.

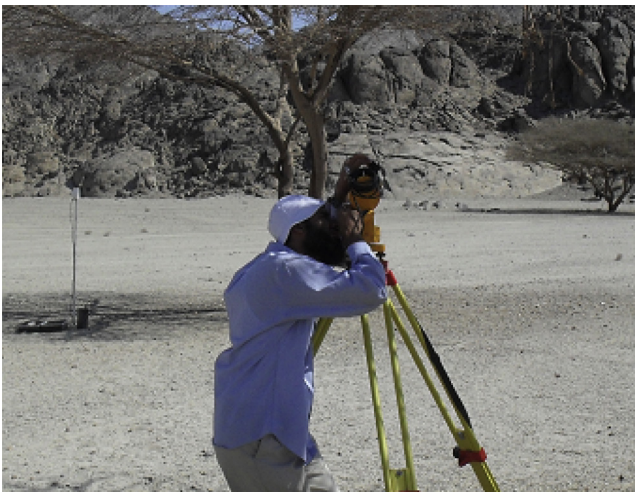


Fig. 5. Solar observation.

The values of the seven magnetic components  $X$ ,  $Y$ ,  $Z$ ,  $F$ ,  $H$ ,  $D$ , and  $I$  at Misallat to the Epoch 2010.0 are 30,766 nT, 2918 nT, 29,870 nT, 42,980 nT, 30,904 nT, 5.418°, 44.25° respectively.

Figs. 6–8 show the maps of the contour lines for the total field intensity  $F$ , the inclination  $I$ , and the declination  $D$  to Epoch 2010.0 respectively.

## 6. The normal magnetic field of Egypt to the Epoch 2010.0 and its secular variation

The area of Egypt is considered relatively small. Thus one central point is sufficient as a reference point for the reduction of the whole measurements performed within the country to obtain the normal field values. El-Menia absolute station (Latitude 28°06.3' N & Longitude 30°45.5' E) is considered as this central point. The measured absolute values of  $F$ ,  $D$ , and  $I$  during the present survey, as well as the calculated values of the Horizontal ( $H$ ), the Vertical ( $Z$ ), the Northward ( $X$ ), and the Eastward ( $Y$ ) components, reduced to the Epoch 2010.0, have been used to compute the Normal Field values in Egypt to the Epoch 2010.0. Taylor's Expansion is used to drive the core field and its secular variation. Referring to Eq. (4), the Taylor expansion to the power 2, in both latitude  $\Phi$  and longitude  $\lambda$  are used to compute the normal elements ( $E_{2010.0}$ ) of the geomagnetic field to the epoch 2010.0

$$E_{2010} = E_0 + a(\Delta\lambda) + b(\Delta\phi)^2 + d(\Delta\phi)(\Delta\lambda) + e(\Delta\lambda)^2 \quad (6)$$

where  $E_0$  is the value of the corresponding element reduced to the Epoch 2010 at El-Menia, ( $a$ ,  $b$ ,  $c$ ,  $d$  and  $e$ ) are constants determined from the field data reduced to the Epoch 2010,  $\Delta\phi = (\phi - \phi_0)$  and  $\Delta\lambda = (\lambda - \lambda_0)$  are the latitude and longitude differences between El-Menia  $\phi_0$ ,  $\lambda_0$  and any point  $\phi$ ,  $\lambda$ . In this way, Eqs. (9)–(15) and Figs. 9–15 are produced to represent the geomagnetic normal field elements to the Epoch 2010.0.

## 7. The standard deviation

The standard deviation ( $\sigma$ ) is calculated for each equation as a measure of how spread out the values. The population standard deviation is the square root of the variance:

$$\sigma = \sqrt{\frac{1}{N} \sum_{i=1}^N (x_i - \bar{x})^2} \quad (7)$$

where  $N$  is the total no. of the coefficient within each equation,  $x_i$  is the geomagnetic element's value and  $\bar{x}$  is simple average.

## 8. The correlation values

To find the correlation value ( $r$ ) between each present geomagnetic value as calculated from  $EGRF_{2010.0}$  equations and the corresponding  $IGRF_{2010.0}$  values at the same points, we chose two profiles across the whole country. The first profile extends in NE-SW direction while the second one extends in N-S direction. Tables 1 and 2 are two examples showing the steps of calculating ( $r$ ) using the known equation:

$$r_{xy} = \frac{\sum_{i=1}^n (x_i - \bar{x})(y_i - \bar{y})}{\sqrt{\sum_{i=1}^n (x_i - \bar{x})^2 \sum_{i=1}^n (y_i - \bar{y})^2}} \quad (8)$$

where  $x_i$  is the value of the geomagnetic element calculated from  $IGRF_{2010.0}$ ,  $\bar{x}$  is the mean of  $x_i$  and  $y_i$  is the value of the geomagnetic element deduced from  $EGRF_{2010.0}$ ,  $\bar{y}$  is the mean of  $y_i$ . The Egyptian Geomagnetic Reference Field (EGRF) equations to the Epoch 2010.0



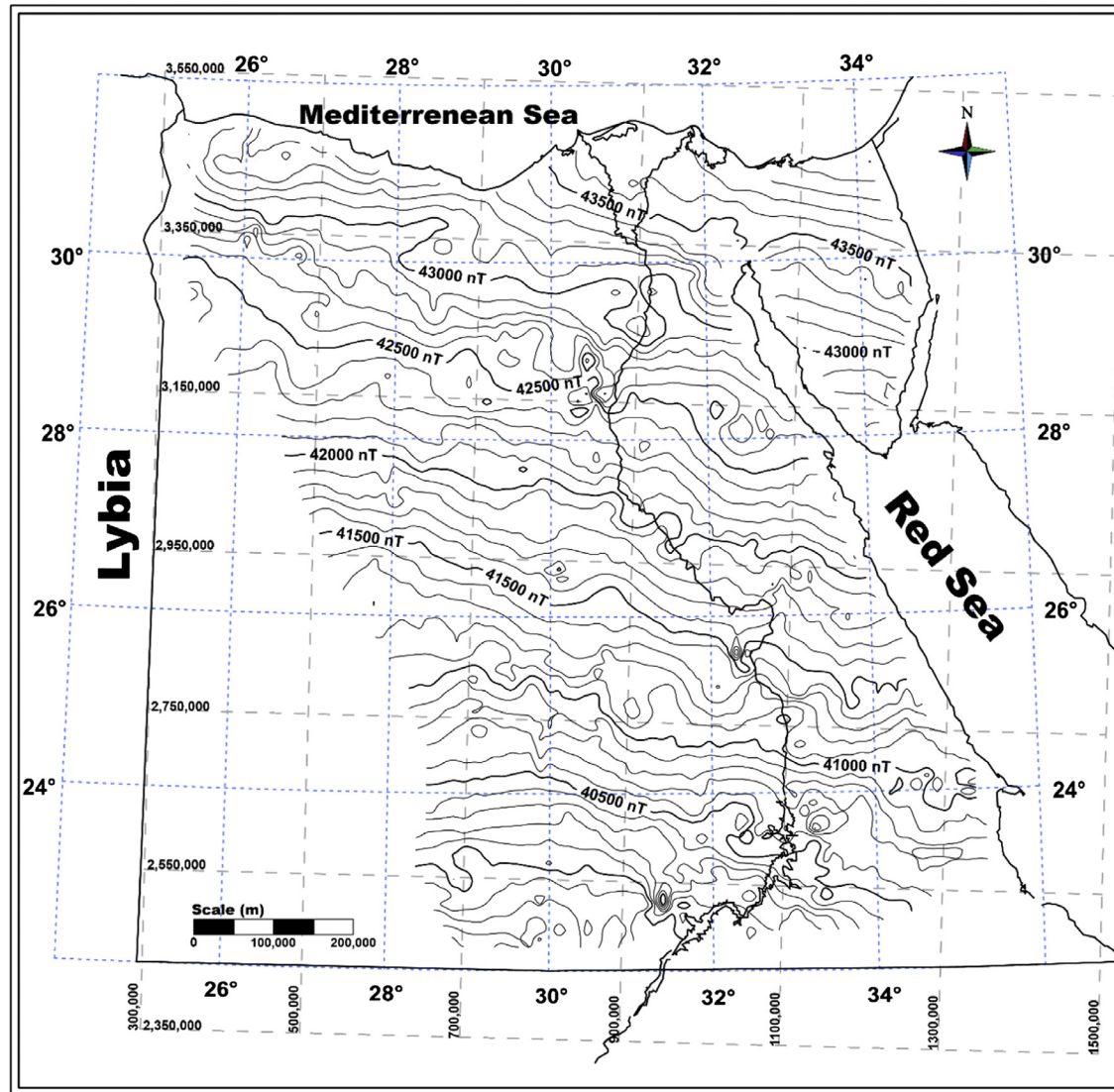


Fig. 6. The total field intensity contour lines (100 nT apart, increasing northward, ranging between 39,500 nT and 44,500 nT With average gradient of about 5 nT/km).

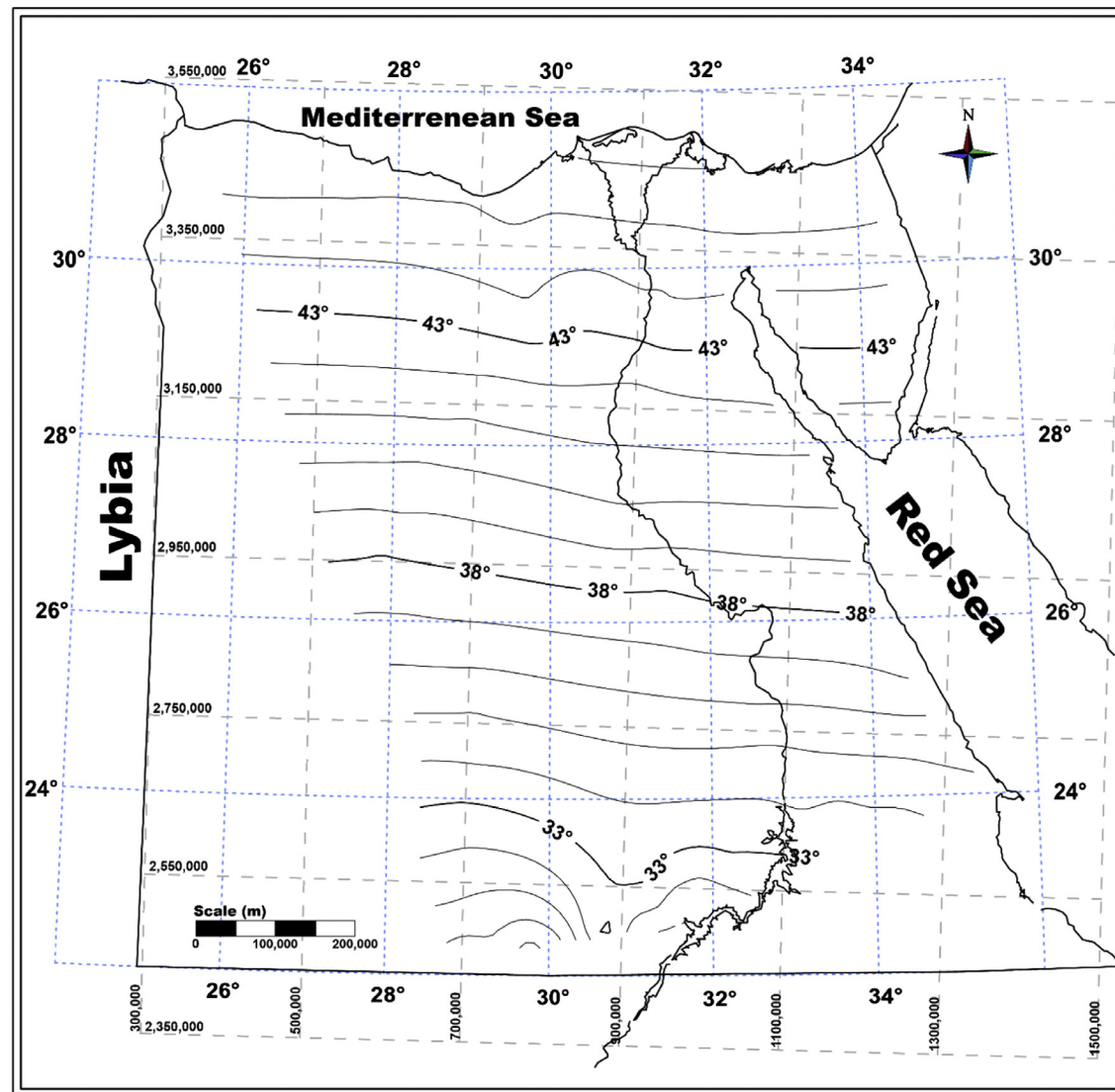


Fig. 7. The geomagnetic inclination contour lines (1.0° Degree apart, increasing northward, ranging between 28° and 47° with average gradient 1.14°/km).



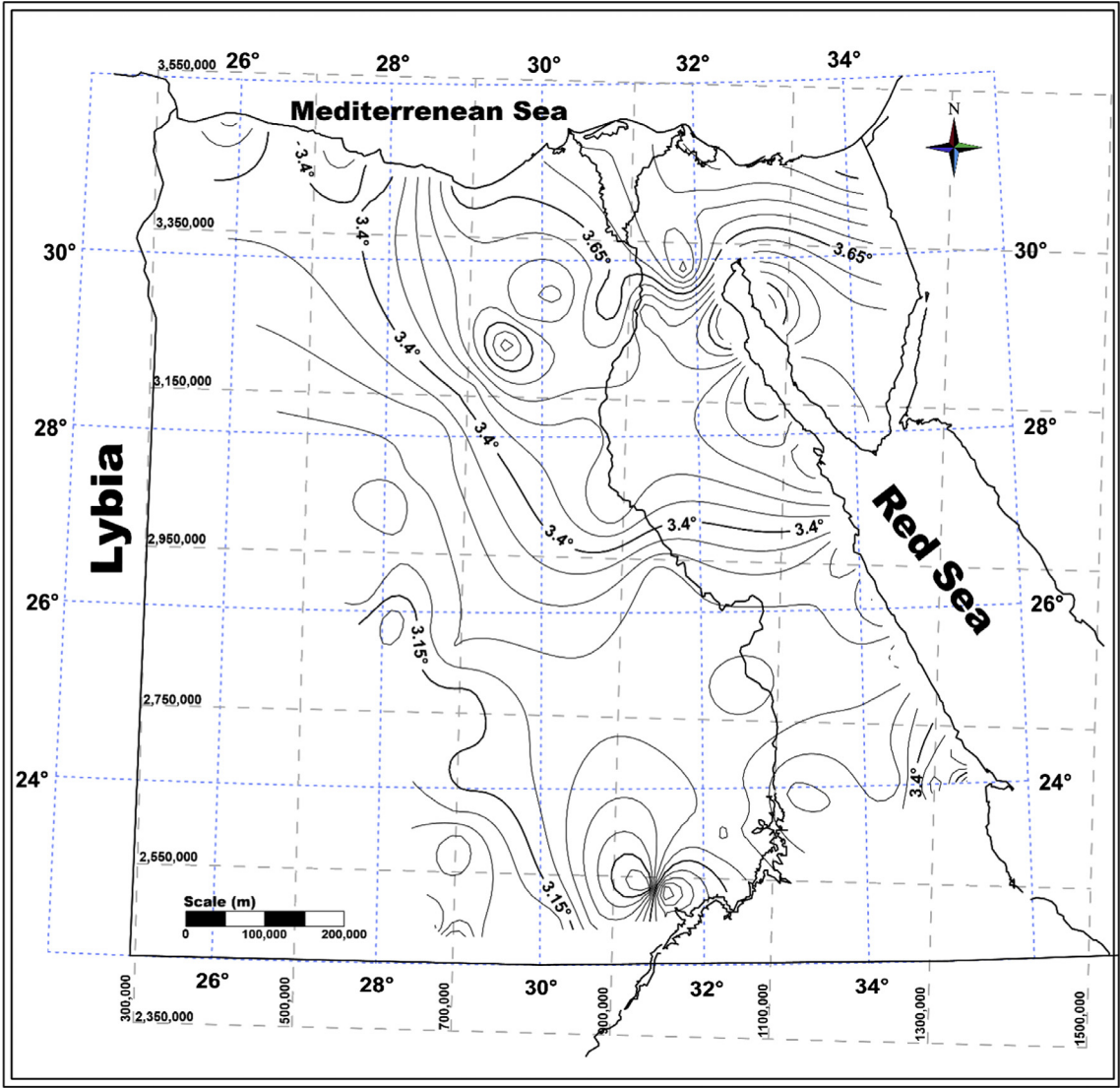


Fig. 8. The geomagnetic declination contour lines (0.05° degree apart, increasing NW SE ranging between 2.4° E and 3.9° E with average gradient 5.4"/km).

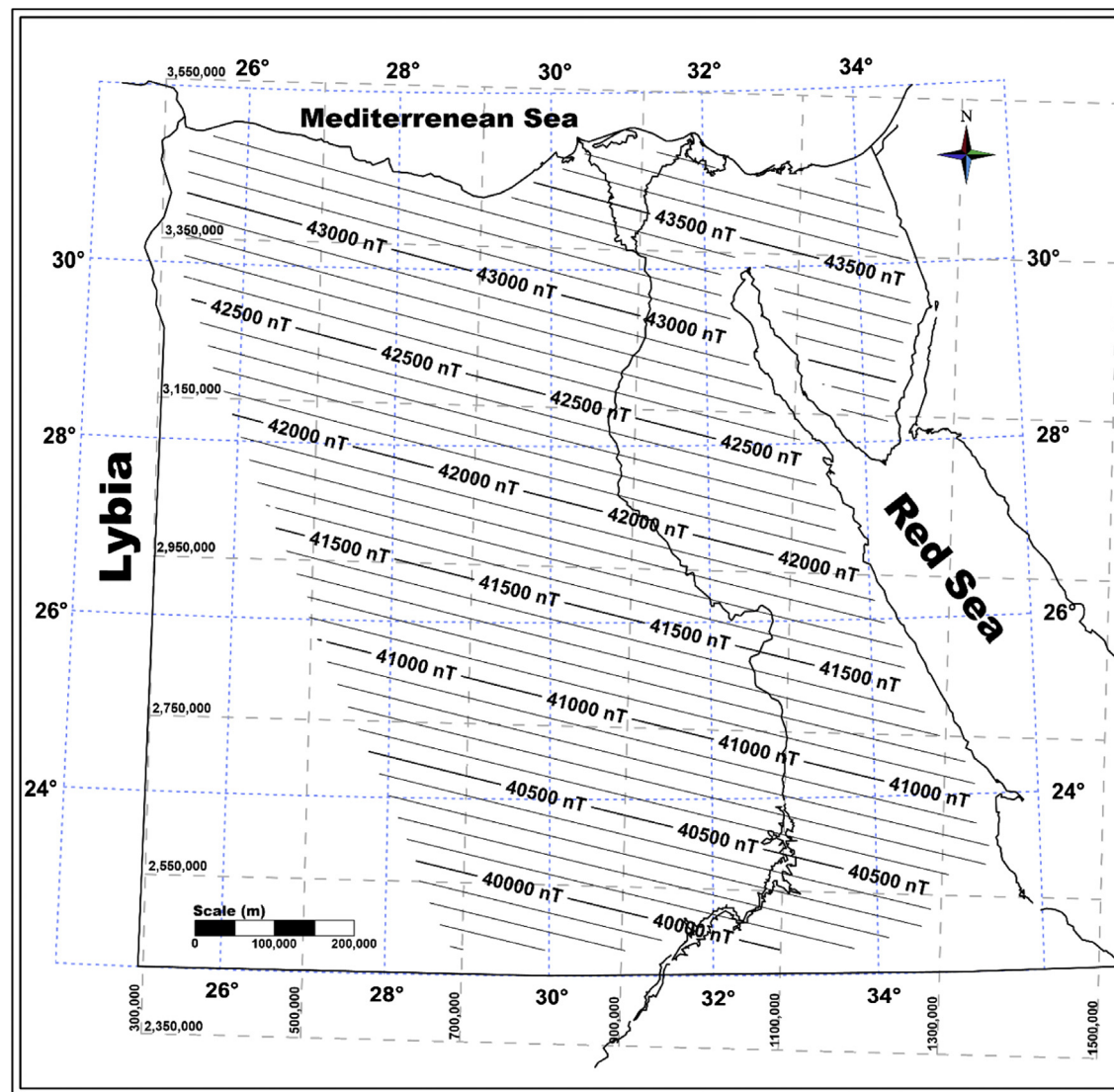
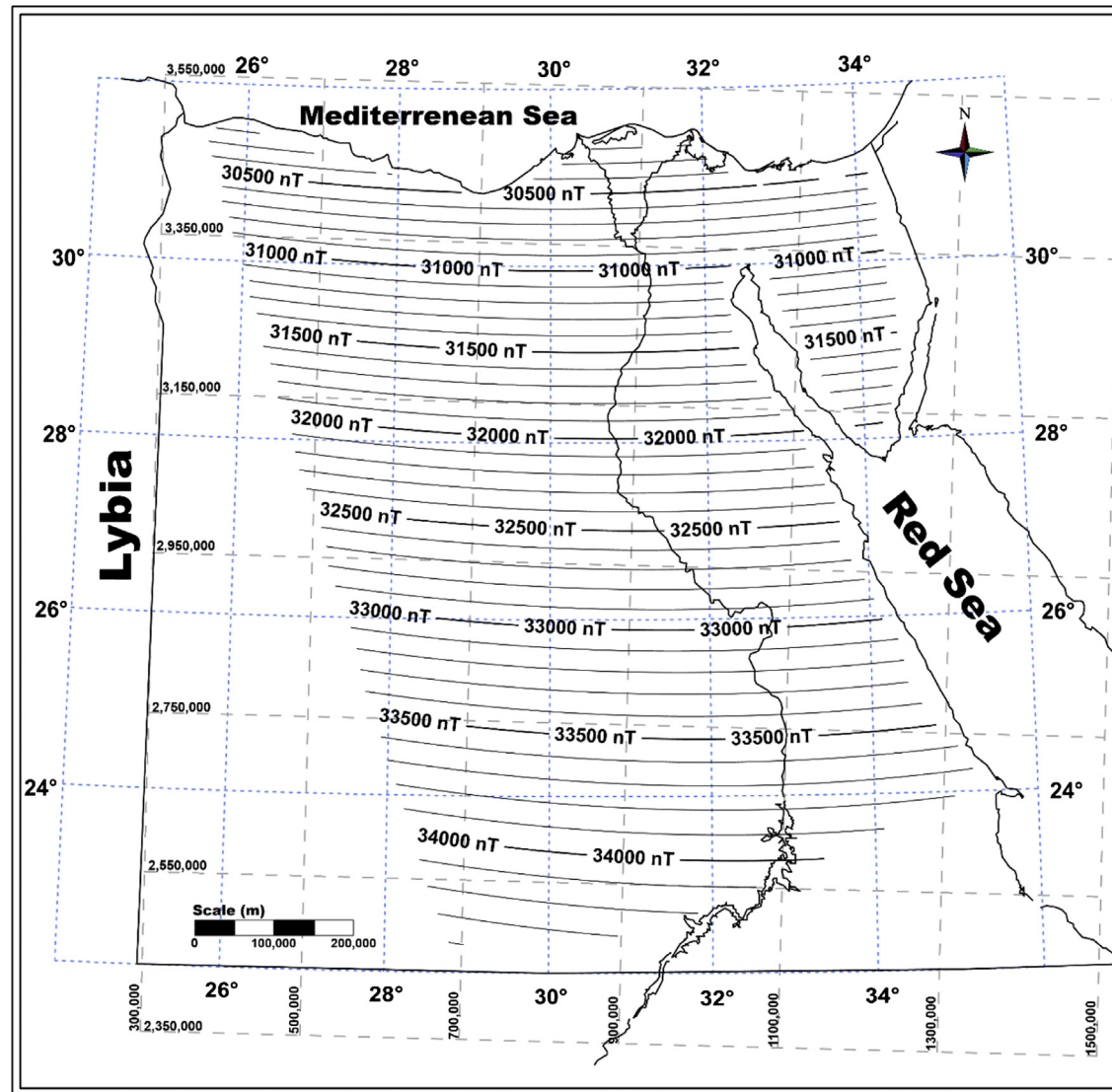


Fig. 9. The normal F contour lines (100 nT apart, increasing towards north-east direction, ranging between 39,500 nT and 44,500 nT with average gradient of about 5 nT/km).





**Fig. 10.** The normal H contour lines (100 nT apart, increasing northward, ranging between 30,000 and 34,600 nT, with average gradient 4.6 nT/km).

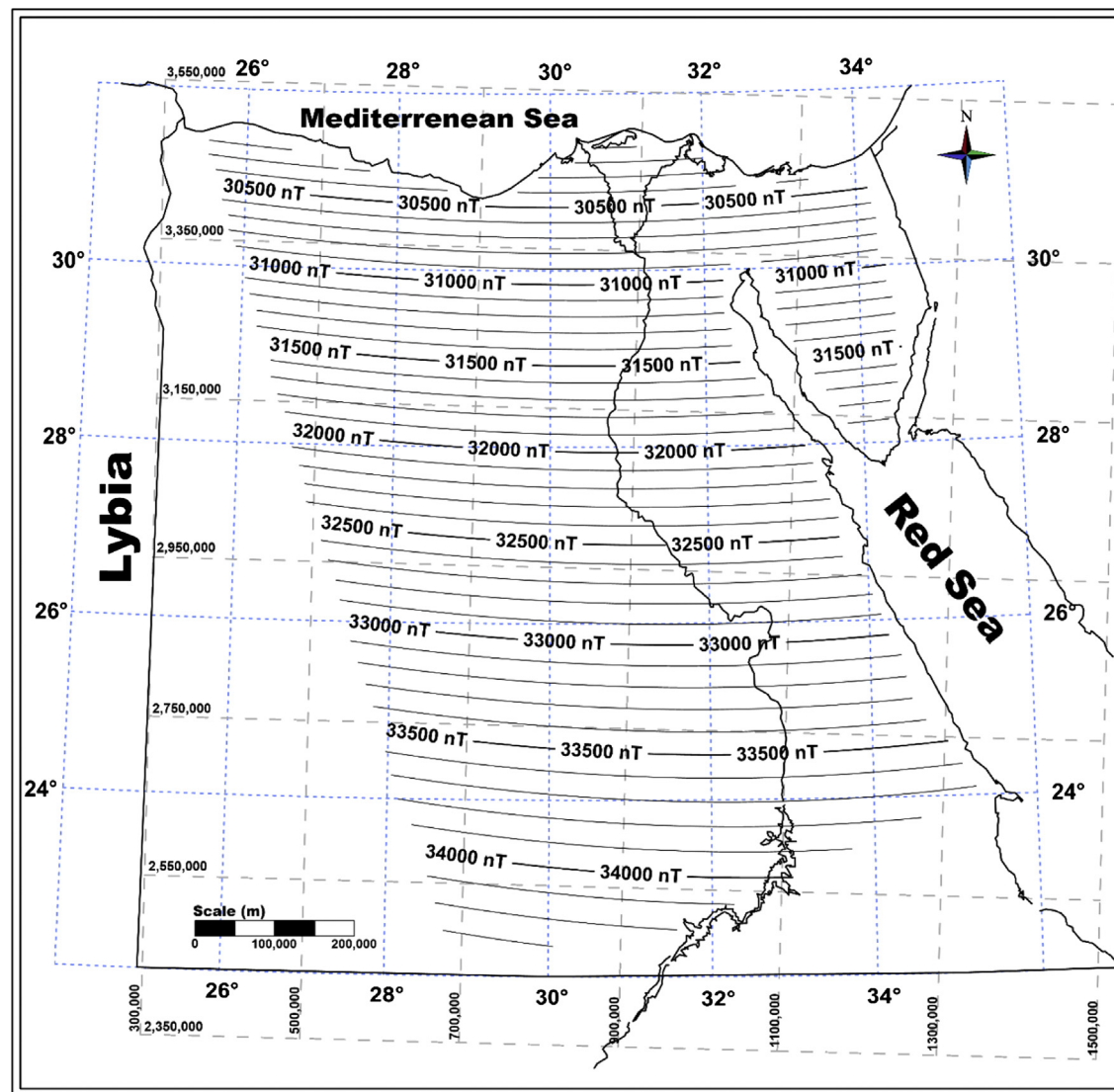
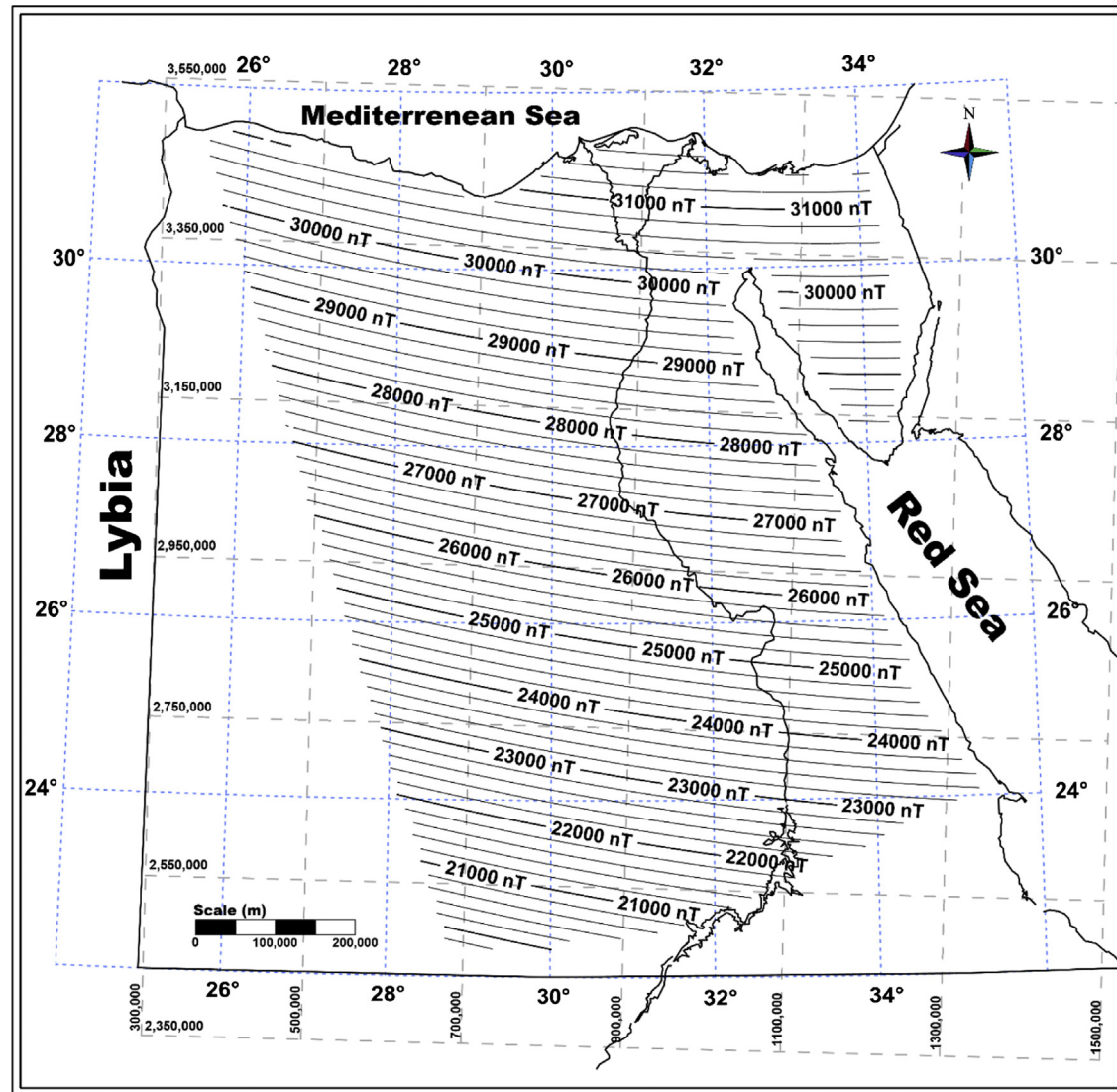
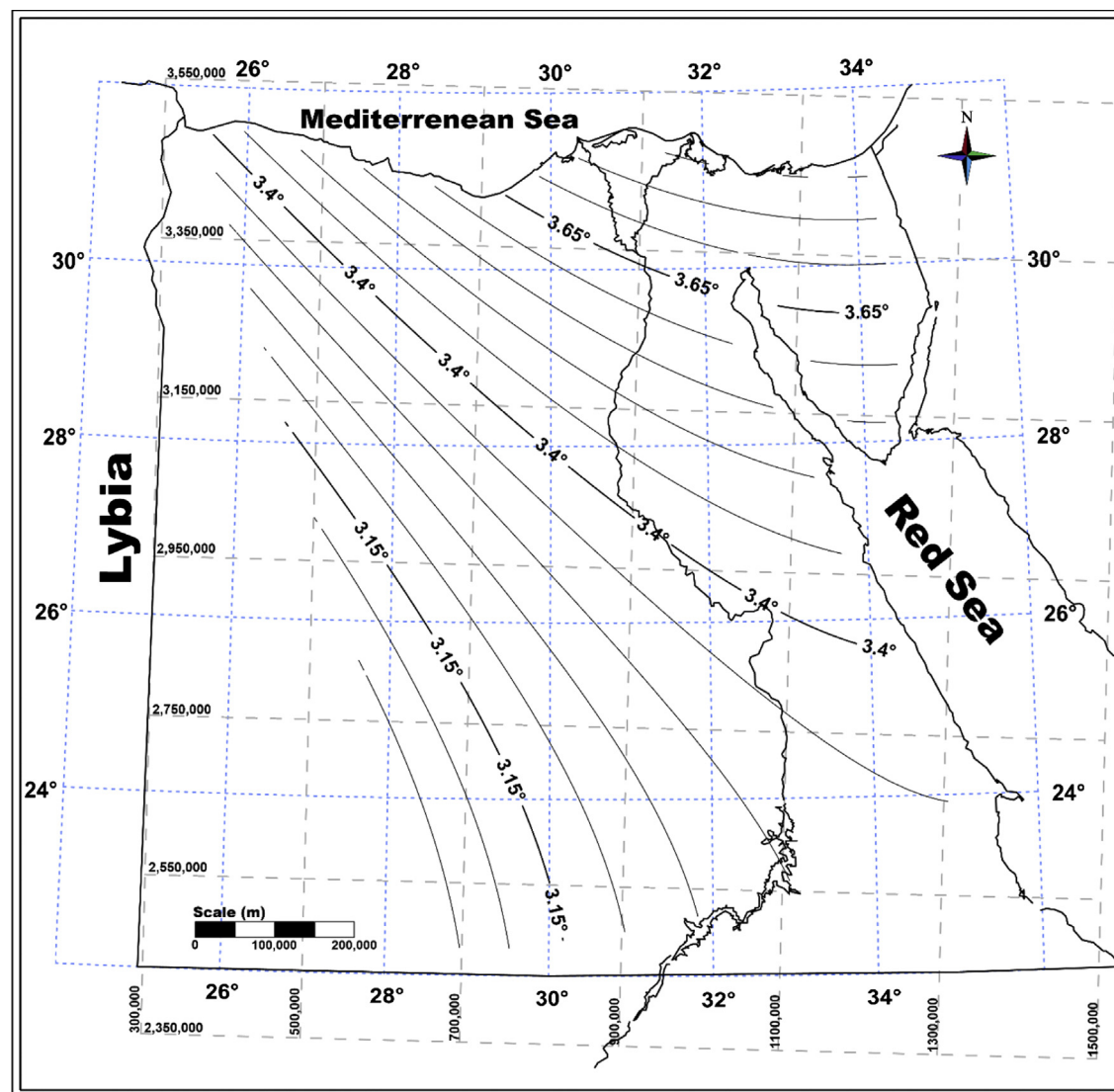


Fig. 11. The normal X contour lines (100 nT apart, increasing northward ranging between 30,000 nT and 34,400 nT with average gradient of about 4.4 nT/km).





**Fig. 12.** The normal Z contour lines (200 nT apart, increasing northward, ranging between 19,000 nT and 32,000 nT with average gradient of 13 nT/km).



**Fig. 13.** The normal D contour lines ( $0.05^\circ$ ) apart, increasing in north-east direction, ranging between  $2.9^\circ$  E and  $4.0^\circ$  E. with average gradient  $3.96''/\text{km}$ .

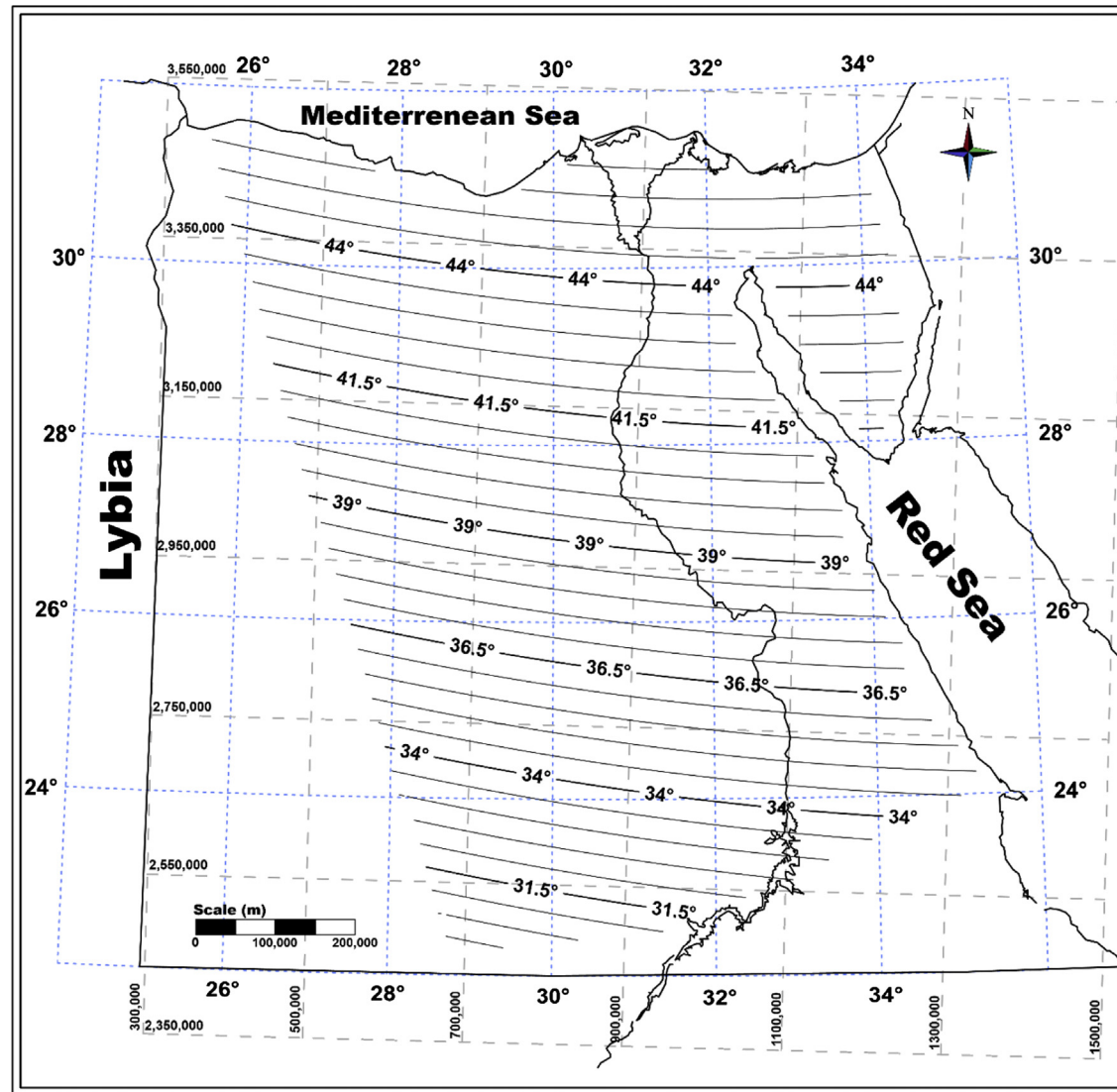


**Fig. 14.** The normal I contour lines (0.5°) apart, increasing northward direction, ranging between 29° and 47° with average gradient of 1.08°/km).



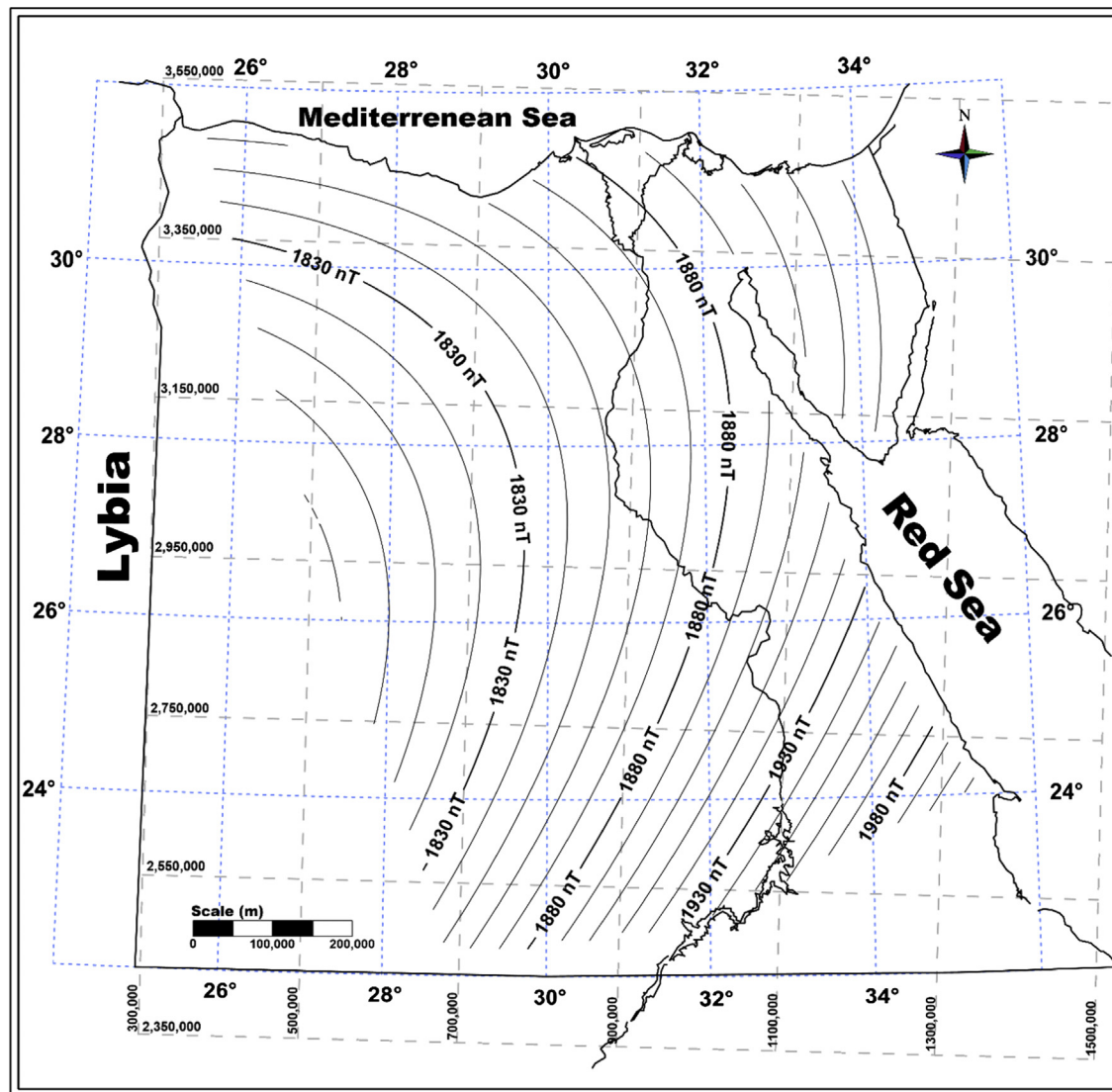


Fig. 15. The normal Y contour lines (10 nT apart, increasing in eastward direction, ranging between 1780 nT and 2020 nT, with average gradient of 0.24 nT/km).

**Table 1**The correlation value between IGRF<sub>2010</sub> and EGRF<sub>2010</sub> for (Y) along NE-SW profile.

(x <sub>i</sub> ) IGRF 1700 nT+	(y <sub>i</sub> ) EGRF 1700 nT	(x <sub>i</sub> - x̄) IGRF- (x)	(y <sub>i</sub> - ȳ) EGRF- (ȳ)	(x <sub>i</sub> - x̄) × (y <sub>i</sub> - ȳ)	(x <sub>i</sub> - x̄) <sup>2</sup>	(y <sub>i</sub> - ȳ) <sup>2</sup>
-38						
23						
77						
125	096	-95	-41	3895	9025	1681
168	110	-52	-27	1404	2704	0729
207	125	-13	-12	0156	0169	0144
242	143	22	06	0132	0484	0036
274	163	54	26	1404	2916	0676
304	185	84	48	4032	7056	2304
333						
363						
1320 (x) = 220	822 (ȳ) = 137			Σ = 11,023	Σ = 22,354	05,570

$$r_{xy} = \frac{\sum_{i=1}^n (x_i - \bar{x})(y_i - \bar{y})}{\sqrt{\sum_{i=1}^n (x_i - \bar{x})^2 \sum_{i=1}^n (y_i - \bar{y})^2}} = \frac{11023}{\sqrt{22354 \times 5570}} = 0.98$$

**Table 2**The correlation value between IGRF<sub>2010</sub> and EGRF<sub>2010</sub> for (F) along N-S profile.

(x <sub>i</sub> ) IGRF 40,000 nT+	(y <sub>i</sub> ) EGRF 40,000 nT+	(x <sub>i</sub> - x̄) IGRF- (x)	(y <sub>i</sub> - ȳ) EGRF- (ȳ)	(x <sub>i</sub> - x̄) × (y <sub>i</sub> - ȳ)	(x <sub>i</sub> - x̄) <sup>2</sup>	(y <sub>i</sub> - ȳ) <sup>2</sup>
0060	0032	-1768	-1770	3,129,360	3,125,824	3,132,900
0503	0484	-1325	-1318	1,746,350	1,755,625	1,737,124
0949	0936	-0879	-0866	761,214	772,641	0,749,956
1394	1381	-0434	-0421	182,714	188,356	0,177,241
1837	1820	0009	0018	162	81	0,000,324
2277	2254	0449	0452	202,948	201,601	0,204,304
2714	2683	0886	0881	780,566	784,996	0,776,161
3145	3107	1317	1305	1,718,685	1,734,489	1,703,025
3569	3525	1741	1723	2,999,743	3,031,081	2,968,729
16,448 (x) = 1828	16,222 (ȳ) = 1802			Σ = 11,521,742	Σ = 11,594,694	Σ = 11,449,764

$$r_{xy} = \frac{\sum_{i=1}^n (x_i - \bar{x})(y_i - \bar{y})}{\sqrt{\sum_{i=1}^n (x_i - \bar{x})^2 \sum_{i=1}^n (y_i - \bar{y})^2}} = \frac{11521742}{\sqrt{11594694 \times 11449764}} = 0.9$$

$$F_{N 2010} = 42379.7 - 465.7(\Delta\lambda_o) + 267.7(\Delta\phi_o) - 15.8(\Delta\phi_o)^2 + 3.9(\Delta\phi_o)(\Delta\lambda_o) + 5.7(\Delta\lambda)^2 \quad (9)$$

$$\sigma = \pm 101.5 \text{ nT}, r = 0.94$$

$$H_{N 2010} = 31419.9 - 467.3(\Delta\lambda_o) - 263.7(\Delta\phi_o) - 15.7(\Delta\phi_o)^2 + 3.9(\Delta\phi_o)(\Delta\lambda_o) + 5.8(\Delta\lambda)^2 \quad (10)$$

$$\sigma = \pm 81.8 \text{ nT}, r = 0.98$$

$$Z_{N 2010} = 28439.9 + 34.5(\Delta\lambda_o) + 589.1(\Delta\phi_o) - 2.6(\Delta\phi_o)^2 - 0.5(\Delta\phi_o)(\Delta\lambda_o) + 1.3(\Delta\lambda)^2 \quad (11)$$

$$\sigma = \pm 102.8 \text{ nT}, r = 0.98$$

$$X_{N 2010} = 31363.0 + 152.5(\Delta\lambda_o) + 302.6(\Delta\phi_o) - 22.6(\Delta\phi_o)^2 - 17.9(\Delta\phi_o)(\Delta\lambda_o) - 4.3(\Delta\lambda)^2 \quad (12)$$

$$\sigma = \pm 81.8 \text{ nT}, r = 0.96$$

$$Y_{N 2010} = 1890.8 + 27.6(\Delta\lambda_o) - 54.5(\Delta\phi_o) + 2.3(\Delta\phi_o)^2 - 2.3(\Delta\phi_o)(\Delta\lambda_o) + 0.9(\Delta\lambda_o)^2 \quad (13)$$

$$\sigma = \pm 4.2 \text{ nT}, r = 0.94$$

$$D_{N 2010} = 3.5^\circ + 0.6^\circ(\Delta\lambda_o) + 0.08^\circ(\Delta\phi_o) + 0.002^\circ(\Delta\phi_o)^2 - .01^\circ(\Delta\phi_o)(\Delta\lambda_o) - .01^\circ(\Delta\lambda_o)^2 \quad (14)$$

$$\sigma = \pm 0.17^\circ r = 0.94$$

$$I_{N 2010} = 42.15^\circ + 1.8^\circ(\Delta\lambda_o) + 4.0^\circ(\Delta\phi_o) - 0.03^\circ(\Delta\phi_o)^2 - 0.02^\circ(\Delta\phi_o)(\Delta\lambda_o) - 0.02^\circ(\Delta\lambda_o)^2 \quad (15)$$

$$\sigma = \pm 4.5^\circ r = 0.98$$

## 9. The Egyptian geomagnetic maps to the Epoch 2010.0

### 9.1. Structural map of Egypt

The Egyptian region is affected by the tectonic plate movement: the African, Arabian, and Mediterranean shields pulling away from each other creating the great rift valley. The figure shows the preliminary structural features of the basement complex in Egypt, as revealed from the analysis of the present magnetic data. More than 60 normal and step faulting systems trending NW-SE affected by the Great African Rift valley and Gulf of Suez, NE-SW systems affected by Gulf of Aqaba, E-W and N-S systems affected by Syrian Arc and the Mediterranean sea. The detailed structural map will be published later by the same authors (see Fig. 16).

The figure implies that:

- (1) The area between Abu-Simble and Aswan contains many active tectonic locations particularly in the vicinity of Toshka where Kalapsha, Sayal, and Karkor faults are located.
- (2) The area between Cairo and El Fayom can be divided in terms of tectonic and geological conditions to two parts: (A) the area between El Fayom and lake Karun is stable area

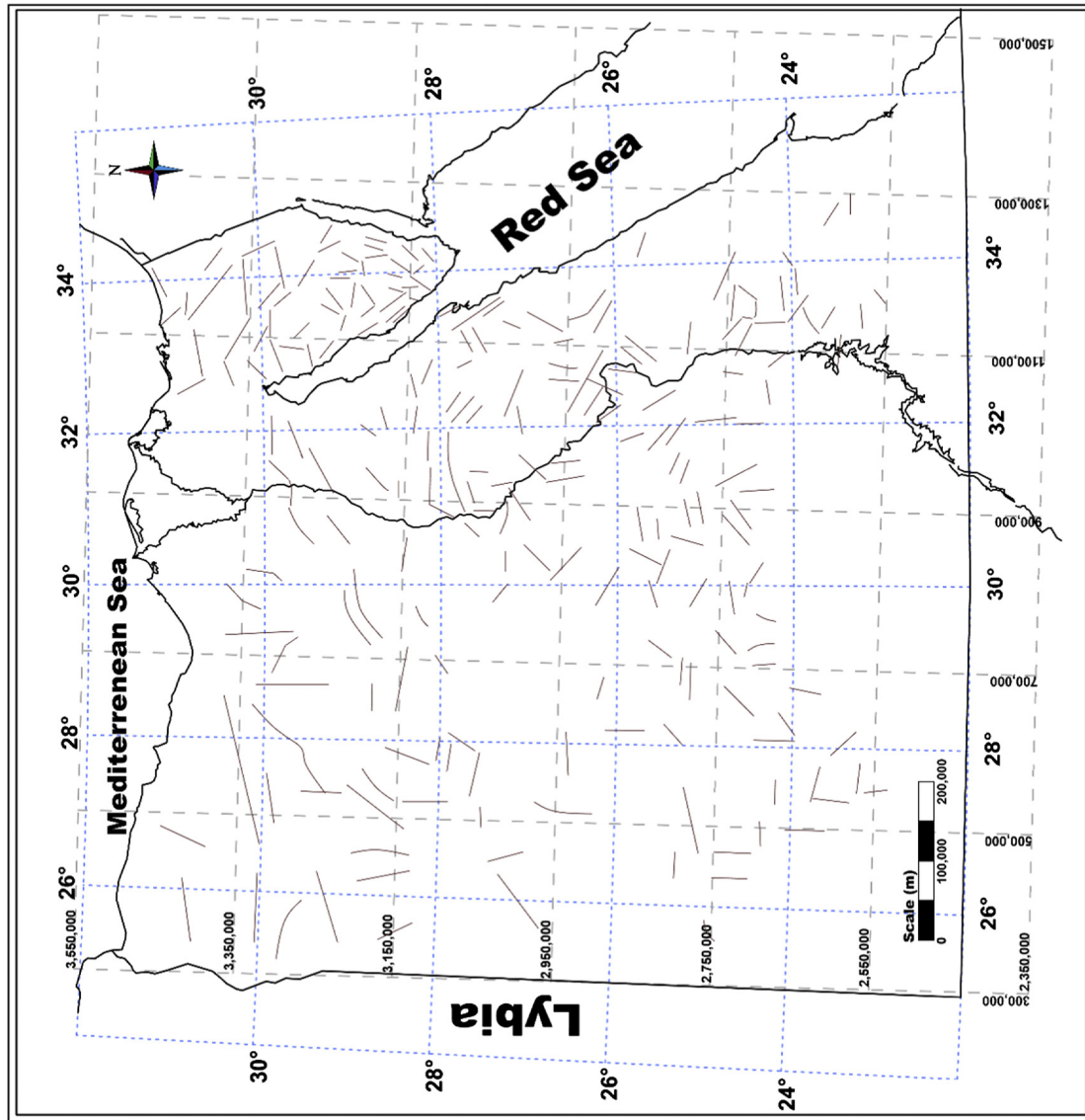


Fig. 16. Structural map of Egypt.



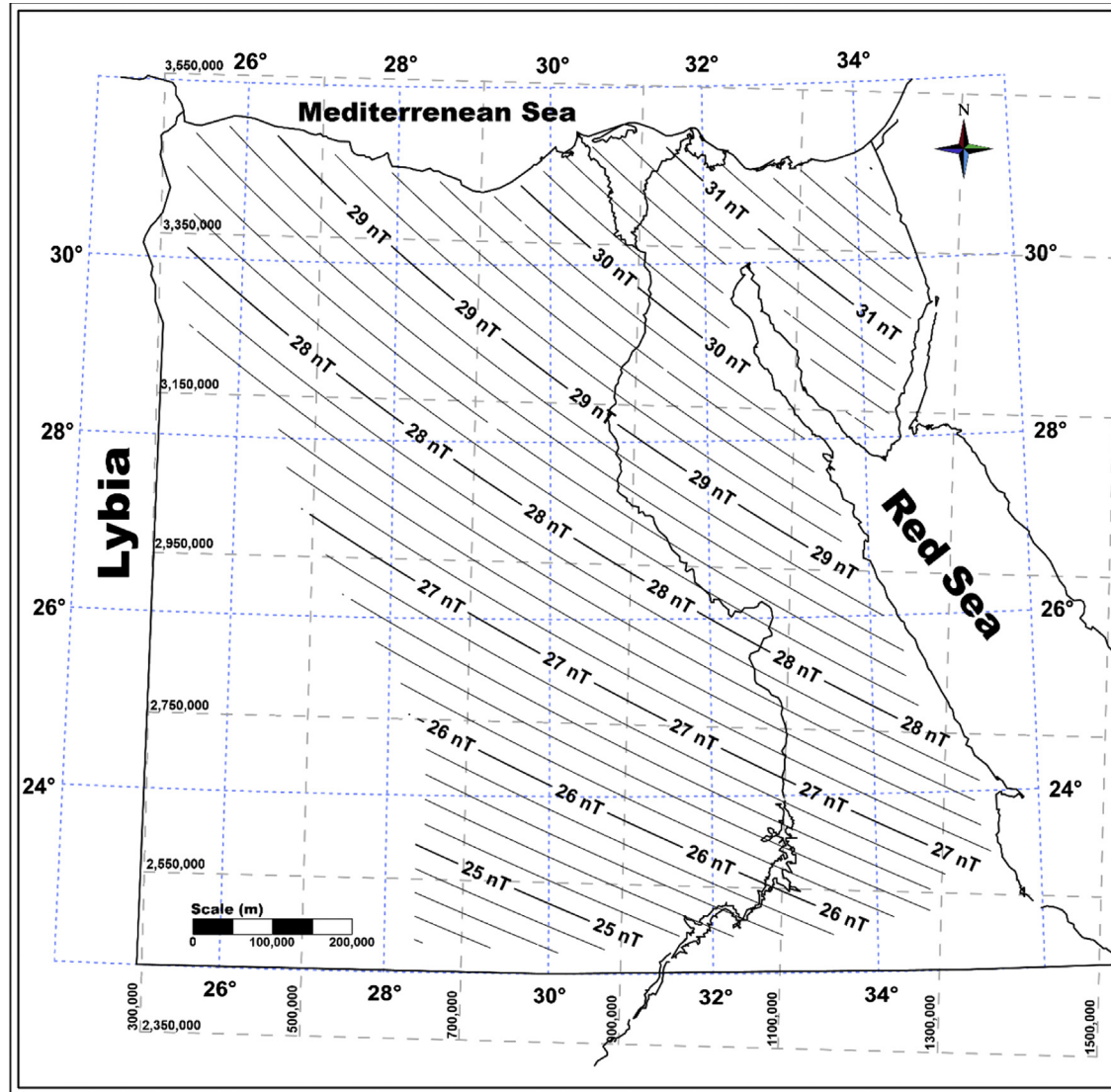


Fig. 17. The secular F contour lines (0.2 nT apart, ranging between 2.4 nT and 32.5 nT).

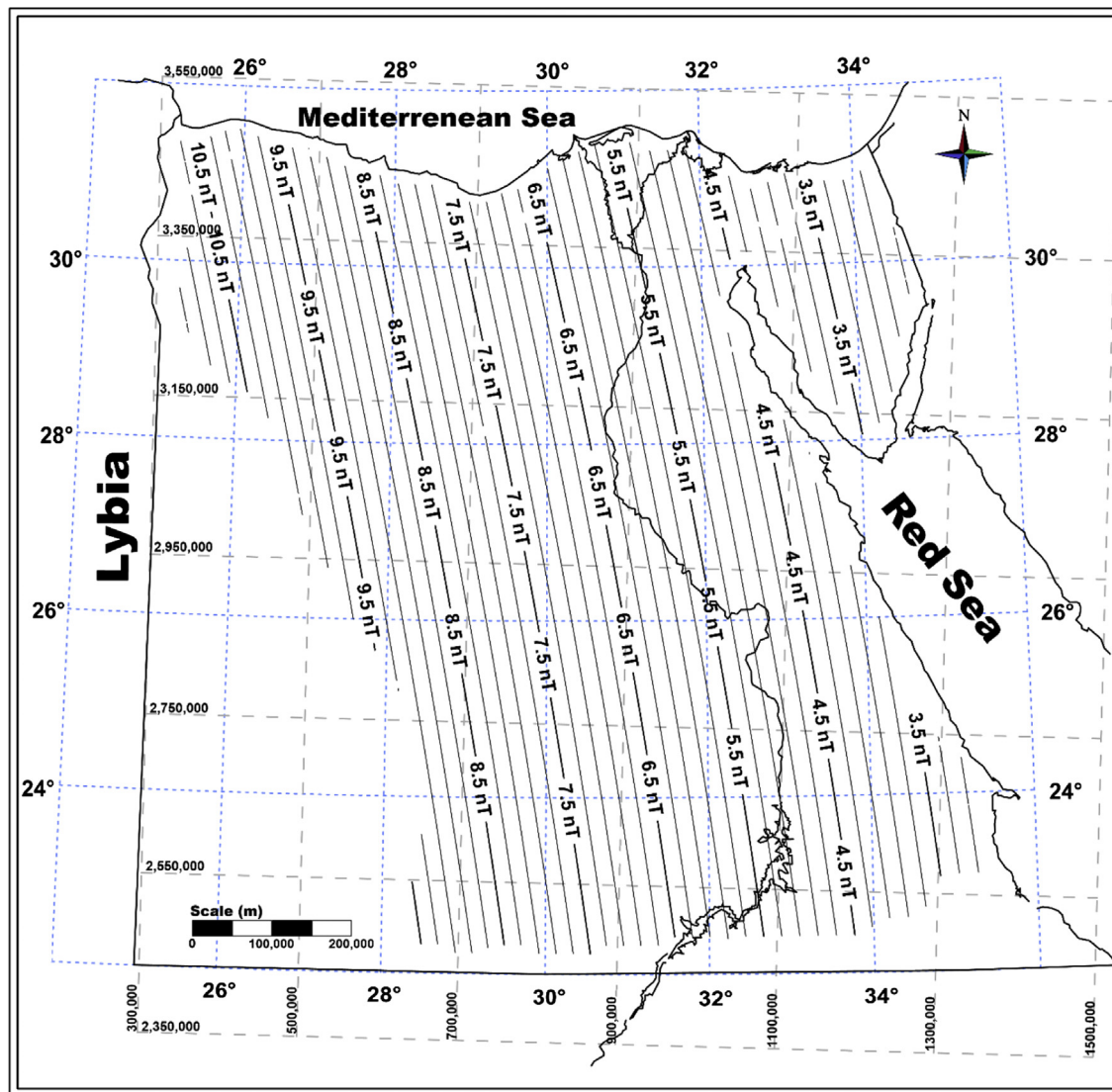


Fig. 18. The secular H contour lines (0.2 nT apart, ranging between 2.5 nT and 11.5 nT).

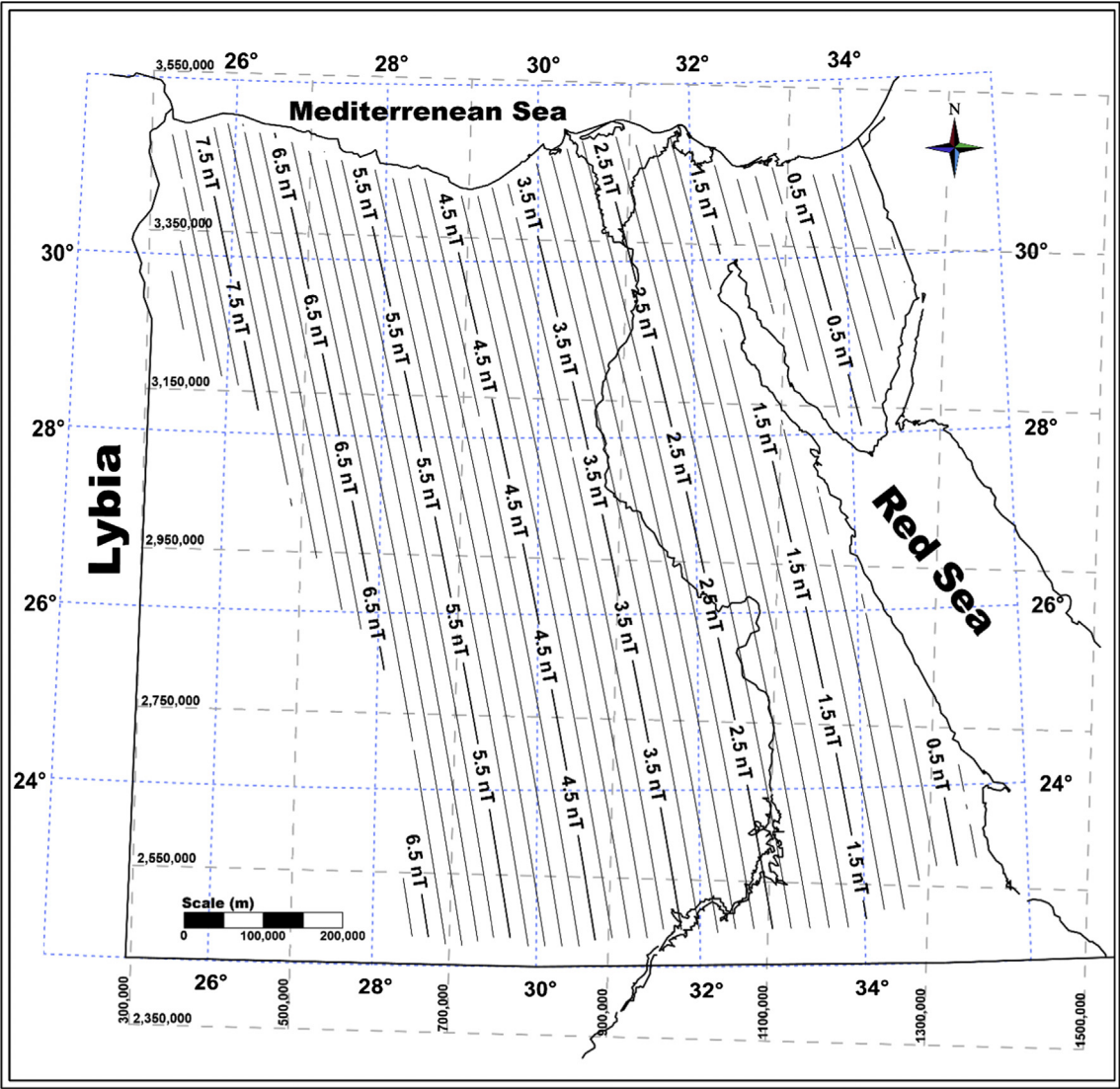


Fig. 19. The secular X contour lines (0.2 nT apart, ranging between 0.5 nT and 8.5 nT).



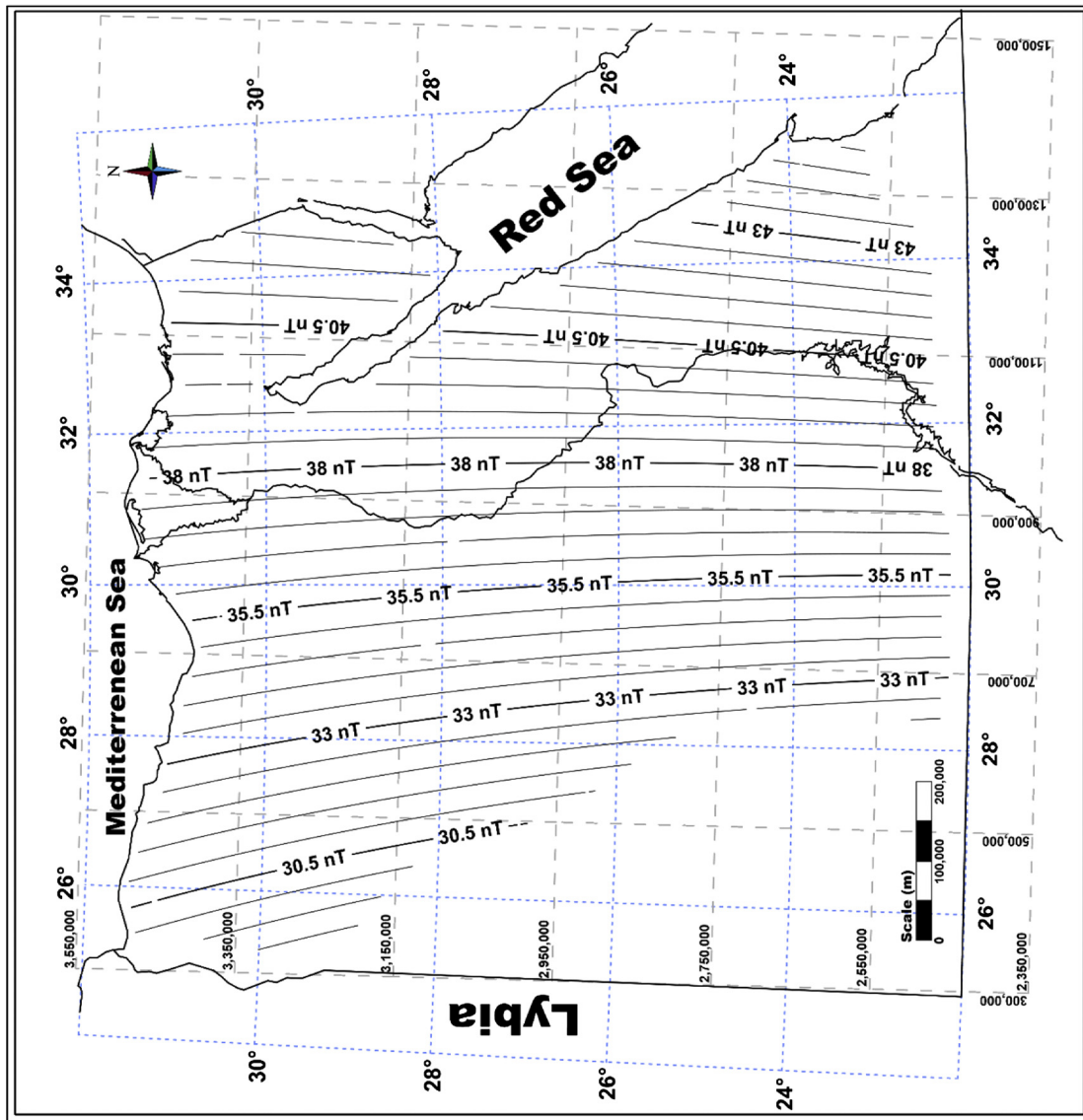


Fig. 20. The secular Z contour lines (0.5 nT apart ranging between 28 nT and 46 nT).

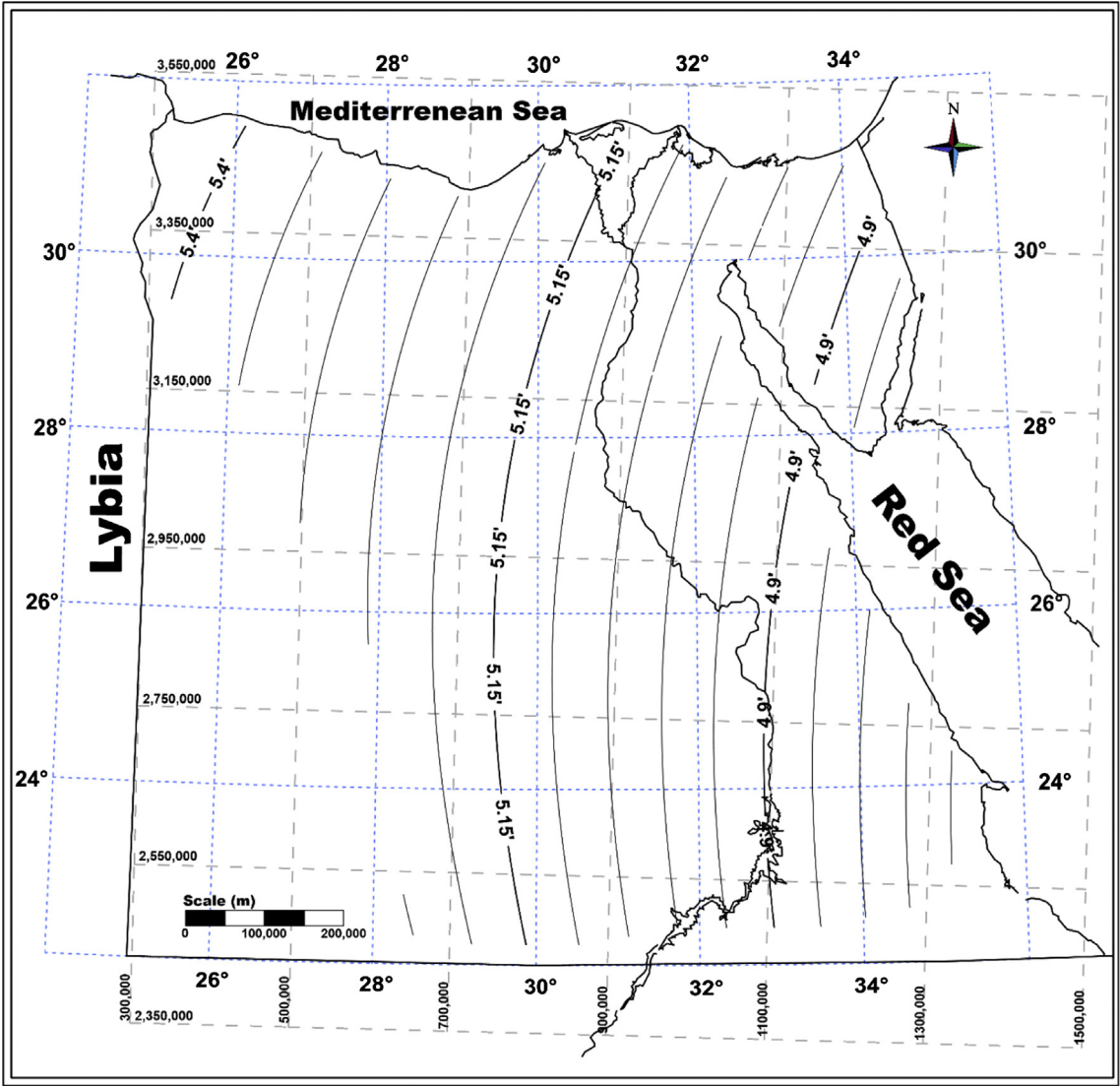


Fig. 21. The secular D contour lines (0.05 min apart, ranging between 4.65 min and 5.45 min).

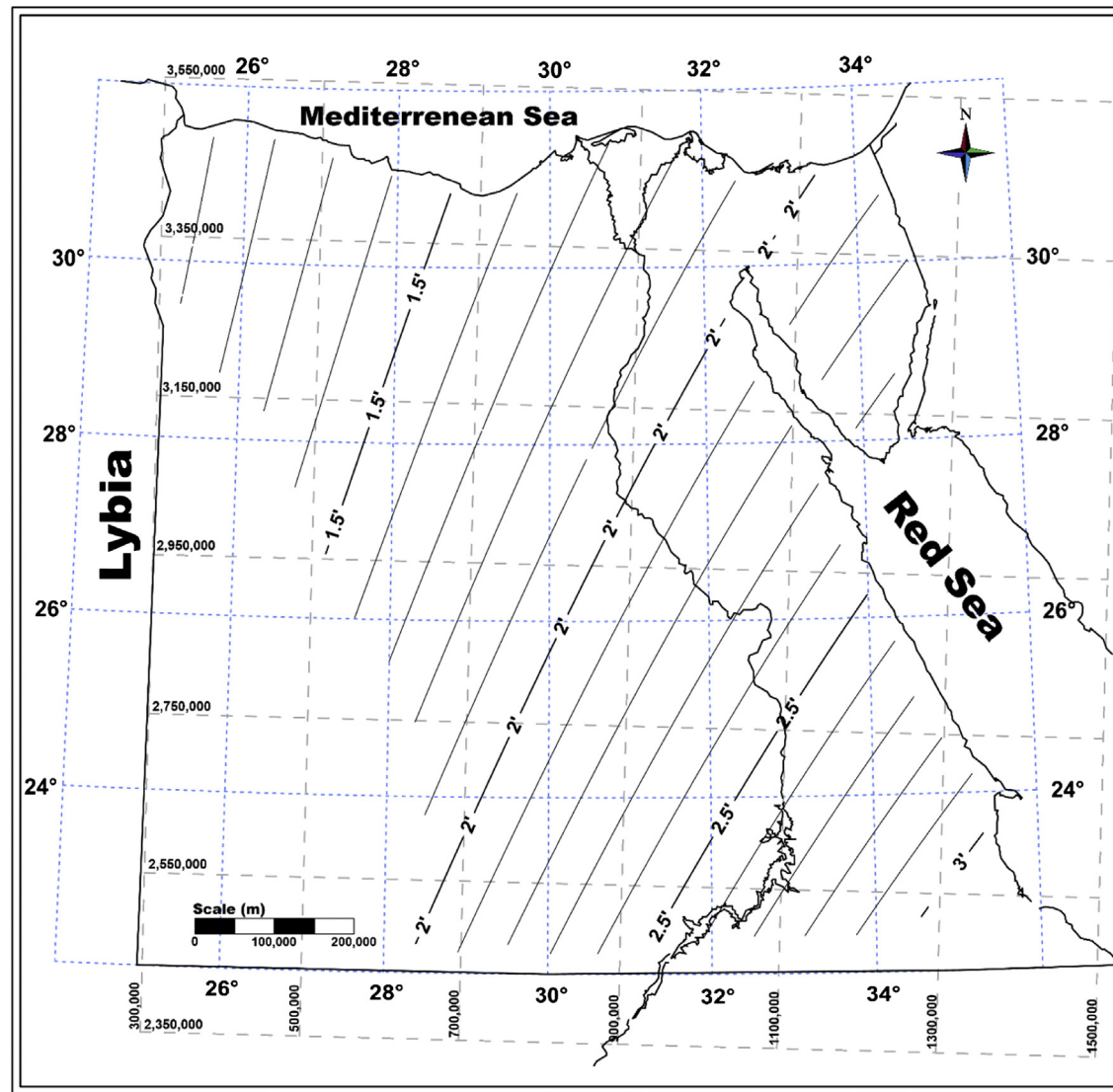


Fig. 22. The secular I contour lines (0.1 min apart, ranging between 1 min and 3.1 min).



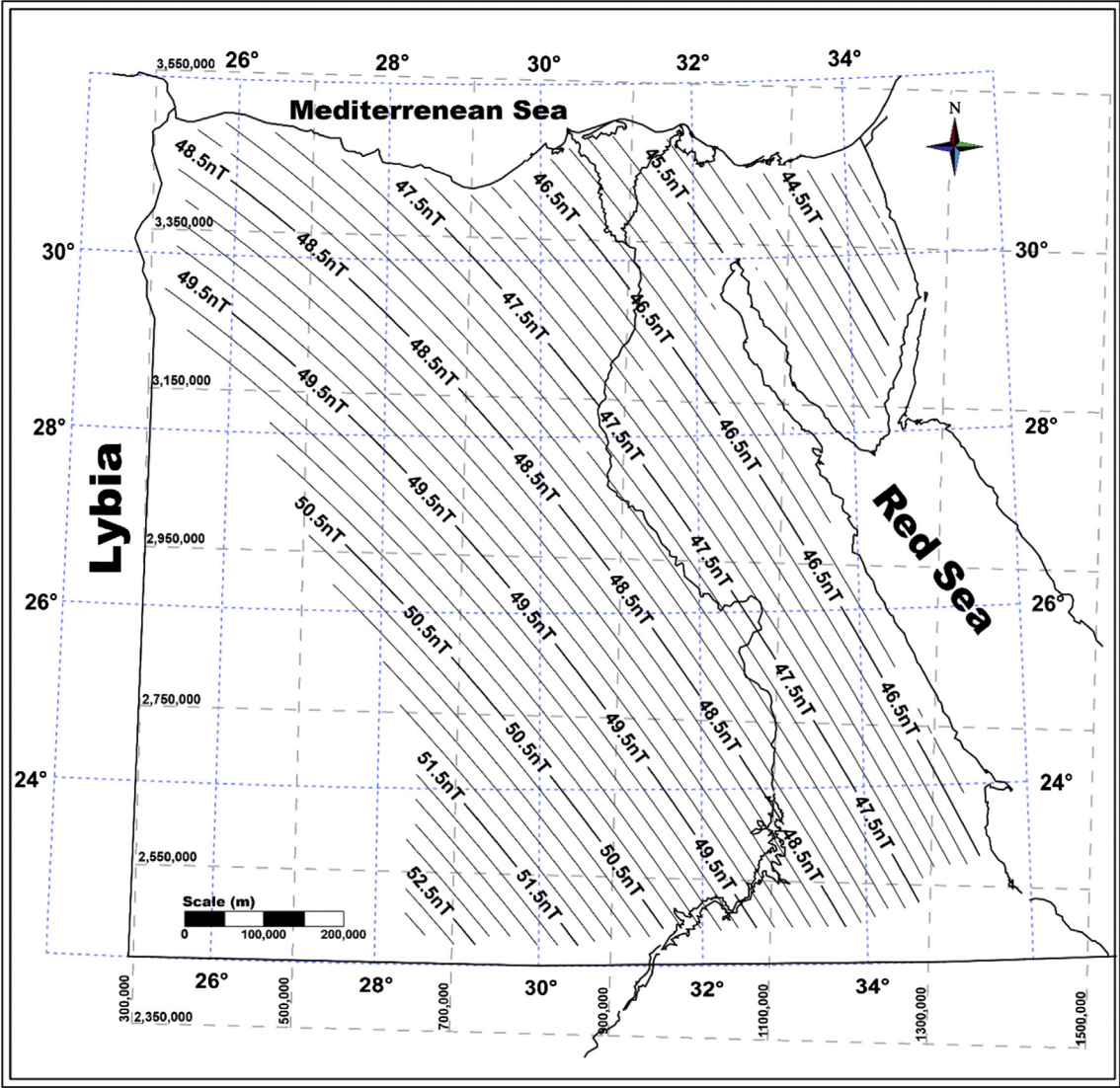


Fig. 23. The secular Y contour lines (0.2 nT apart, ranging between 43.5 nT and 53.5 nT).

and suitable for urban development in addition to the fact that the necessary water can be obtained from Bahr Youssef. (B) Dahshur area and along about 30 miles in the direction of El Fayom is characterized as an active tectonic area due to the presense of Dahshur fault with inclination angle of about 35 angle towards the SE-NW.

- (3) Basalt eruptions spread at a number of areas around El kharga-East El owinat, East El owinat - Abu-Simble, and Abu-Simble - Aswan roads.
- (4) Many areas are characterized as stable areas and have enough sources of water. These areas are legible for the extension of the near cities.

The obtained data is integrated by the authors and other members of the project's team (Esmat et al., 2013) with other geophysical data to study the subsurface structure, the tectonic situation and the stability of the anomalous regions.

## 9.2. The secular magnetic variation in Egypt

For any point, the annual rate of change for any element  $\partial M/\partial t$  for any Epoch  $t$ , could be computed to any Epoch according to the formula (Ibrahim, 1971)

$$M_t = a + bt + ct^2 \quad (16)$$

where (a, b and c) are constants. If these values for several points are determined, a Taylor expansion to the power two in latitude and longitude could be used to obtain the normal distribution of the secular variation within the region. 50 absolute stations that had been occupied by earlier observers are used to calculate the secular variation. Comparing the data for each of these stations, the annual rate of change of the geomagnetic element  $\partial M/\partial t$  is computed for the elements ( $F, D, I, X, Y, Z$  and  $H$ ). Taking El-Minya as central point, ( $\lambda_0 = 30^\circ 45.5'$ ,  $\phi = 28^\circ 06.30'$ ), the least square technique is used to calculate the coefficients (a, b, and c) in the linear function:

$$\partial M/\partial t = a + b(\Delta\lambda) + c(\Delta\phi) \quad (17)$$

where ( $\Delta\lambda$  and  $\Delta\phi$ ) are the differences in longitude and latitude between El-Minya and the station. The following Eqs. (18)–(24) and Figs. 17–23 are obtained for the different geomagnetic elements.

$$\partial F/\partial t = 2.704 + 0.265(\Delta\lambda) + 1.140(\Delta\phi)\text{nT}, \quad (18)$$

$$\partial D/\partial t = 9.209 + 0.021(\Delta\lambda) + 1.140(\Delta\phi)\text{min} \quad (19)$$

$$\partial I/\partial t = 6.457 + 0.456(\Delta\lambda) + 0.028(\Delta\phi)\text{min} \quad (20)$$

$$\partial X/\partial t = 55.904 + 2.0130(\Delta\lambda) + 0.200(\Delta\phi)\text{nT} \quad (21)$$

$$\partial Y/\partial t = 97.161 + 0.136(\Delta\lambda) + 0.007(\Delta\phi)\text{nT} \quad (22)$$

$$\partial Z/\partial t = 84.345 + 4.559(\Delta\lambda) + 1.857(\Delta\phi)\text{nT} \quad (23)$$

$$\partial H/\partial t = 54.036 + 1.795(\Delta\lambda) + 0.257(\Delta\phi)\text{nT} \quad (24)$$

## 10. Conclusion & Recommendation

- (1) The correlation values ( $r$ ) between IGRF<sub>2010.0</sub> and EGRF<sub>2010.0</sub> are almost 0.9 for nearly all the geomagnetic elements. The differences between the geomagnetic elements as calculated from the two references are nearly steady ranging around 50 nT, which may be due to the ionosphere condition at the region.

- (2) The subsurface structure in Egypt is affected mainly by the Great African Rift Valley, the opening of the Red Sea at Ras Mohammed into the Suez and Aqaba Gulfs, and the Syryan arc.
- (3) The stable areas near the cities, having enough sources of water, are legible for urban development and new housing extension as examples near Abu-Simble city, Aswan city in the direction of El Oxser, Kharga city in the direction of East El Owinat, and the area around East El Owinat in the direction of Abu-Simble. These areas will be subjected to detailed measurements to study the subsurface structure there and their fitness for housing, reclamation, and civil engineering.

## Acknowledgment

This paper has been supported by the Egyptian Science and Technology Development Fund program (STDF) through research project "Geomagnetic Survey & Detailed Geomagnetic Measurements within the Egyptian Territory" (ID 1275).

The authors wish to express their thanks to Prof. Dr. Mohammed Al-saed, Prof. Dr. Ibrahim El-Hemaly, Dr. Mahmod Mekki, Prof. Dr. Taha Rabeh, and Dr. Maha Abdelazem of the Geomagnetic laboratory, NRIAG, for their valuable help in the field measurements as well as in the computation of the data.

Thanks are also due to Prof. Dr. Fath-Elbary R. the head of Aswan Regional Earthquak Centre, and to Engineer Mohammed Ibrahim the head of Aswan High Dam Authority for their helpful facilities introduced to the team of measurements during the geomagnetic marine survey of Naser Lake.

## References

- Abdelkhalek, M.L., Abdel Wahed, N., Sehim, A.A., 1993. Wrenching deformation and tectonic setting of the northwestern part of the Gulf of Suez. *Geol. Soc. Egypt special Pub.*
- Barracough, D.R., 1987. International geomagnetic reference field: the fourth generation. *Phys. Earth Planet. Inter.* 48 (279), 292.
- Bucha, Václav, 1957. "Normál ní geomagnetické pole vertkáln složky V Českykychénúch kb epše 1950.0" *Československá Akad. Věd Geofys. Ústav Práce Geofys. Sborník*, no. 51, pp. 577–600.
- Campbell, W.H., 1997. *Introduction to Geomagnetic Fields*. Syndicate Press of the University of Cambridge.
- Carnegie Institution of Washington, 1920. *Researches of the Dep. Of Terrestrial Magnetism* (Carnegie Institution Pub. No. 175, V. 4.).
- Chapman, S., Bartels, J., 1940. *Geomagnetism*, vol. 2. Clarendon Press, Oxford, p. 1049.
- Deebes, H., Fahim, M., Ahmed, F., 1978. The Geomagnetic Total Intensity & the Inclination of Egypt Reduced Institute of Astronomy and Geophysics, Bulletin No. 164.
- Deebes, H., Ahmed, F., 1979. Micro Magnetic Survey of the Area North East of Qena. Helwan Institute of Astronomy and Geophysics, Bulletin No. 205.
- Deebes, H., Hussain, A.G., Fahim, M., Ahmed, F., 1980. Maps of the Absolute Geomagnetic Field Components of the Eastern Desert of Egypt Reduced to the Epoch 1977.0. Helwan Institute of Astronomy and Geophysics, Bulletin No. 218.
- Deebes, H., 2012. Seismotectonics of South Sinai, Egypt. *Gulf Seismic Forum*, Saudi Arabia.
- Esmat, M., Geomagnetic laboratory member, 2013. Geomagnetic Survey & detailed Geomagnetic Measurements. Final report of project (ID 1275) funded by the Egyptian Science and Technology Development Fund program (STDF).
- Fahim, M., Wienert, K., 1958. Magnetic Survey Work in Egypt) (Helwan Observatory Bulletin No. 46.).
- Fahim, M., 1968. Magnetic Survey of U. A. R. Reduced to Epoch 1965.0 (Helwan institute of Astronomy and Geophysics, Bulletin no. 79).
- Hurst, H.E., 1915. The Magnetic Survey of Egypt and the Sudan. Ministry of Finance, Egypt Survey Department, paper No. 33.
- Ibrahim, Ezz-Eldin M., 1971. The normal geomagnetic field of U. A. R. for the Epoch 1965.0 and its secular variation. Thesis submitted to faculty of science, Cairo University.
- Issawi, Bahay, El-Hinnawi, M., Francis, M., Mazhar, A., 1999. The phanerozoic geology of Egypt, a geodynamic approach. The Egyptian geological survey, special publication no. 76.

- Keeling, B.F.E., 1907. Magnetic observations in Egypt 1895–1905 with a summary of previous magnetic work in northern Africa. Survey department paper no. 6.
- Lyons, C., 1910. Magnetic Observations in Egypt (Proc. Roy. Soc. Vol. 71).
- Madwar, M.R., 1954. Magnetic observation in the Sudan Jan.-Feb. 1952. Bull. De L'Institute d' Egypte V. 36.
- Neev, D., 1975. Tectonic evolution of the Middle East and the Levantine basin (eastern most Mediterranean). *Geology* 3, 683–686.
- Parkinson, W.D., 1983. *Introduction to Geomagnetism*. Scottish Academic Press, Edinburgh and London, p. 433.
- Rabeh, T., 2003. Structural set-up of Southern Sinai and Gulf of Suez areas indicated by Geophysical data. *Ann. Geophys.* 46 (6), 1325–1337.
- Said, R., 1990. The Geology of Egypt, second ed., pp. 439–449.
- Wienert, K.A., 1970. Notes on Geomagnetic Observatory and Survey Practice. Published by UNESCO, Printed in Belgium.